Norwegian University of Life Sciences
Faculty of Veterinary Medicine and Biosciences

Department of Chemistry, Biotechnology and Food Science

Master Thesis 2015
60 credits

Effect of Ammonia on Metabolic Activity, Urea Production and Gene Expression in Hepatocytes

Karianne Vegheim

2015

Effect of Ammonia on Metabolic Activity, Urea Production and Gene Expression in Hepatocytes

Karianne Vegheim

http://brage.bibsys.no/umb/

Acknowledgement

This thesis is a final work of a master degree in biotechnology at the Norwegian University of Life Sciences. The work is performed at the Department of Pediatric Research Institute, Rikshospitalet, Oslo University Hospital, from June 2014 to May 2015.

My sincere thanks goes to my supervisor Runar Almaas, MD, PhD for giving me the opportunity to take part in his science. Runar, your engagement, knowledge, and advices have been priceless. I am very grateful!

I would also like to thank Professor Tor Erling Lea for being my internal supervisor.

I wish to express an extra gratitude to the amazing Monica Atneosen-Åsegg, Grethe Dyrhaug, and Camilla Schjalm. Thank you for teaching me laboratory techniques, and sharing your experience. I really appreciate it!

I would also like to thank everyone at PFI, and Professor Ola Didrik Saugstad, for giving me permission to perform my master thesis at the department.

Further I will like to express my gratitude to Dr. Gareth Sullivan and Richard Siller at Institute of Basic Medical Sciences, University of Oslo, for kindly providing stem cell, and Astrid Steiro and Helge Rootwelt at the department of Medical Biochemistry, for allowing me to analyse samples. Thank you!

Finally, to the most important and incredible people in my life, family & friends! Thank you for always encouraging me, for cheering me on, and for making me hundreds of cups with fresh coffee! I am honored that I get to be a part of your lives, cause you are for sure coloring mine. I love you!

Ås, May 15th, 2015

Karianne Vegheim

Abstract

Background: The key organ for ammonia detoxification is the liver, predominantly via urea cycle and glutamate-glutamine cycle. In patients with acute and chronic liver failure, hyperammonemia often occur as a secondary condition. Elevated blood ammonia levels give arise to increased ammonia concentration in the brain, which can result in hepatic encephalopathy and hepatic coma. While the neurotoxic effects of increased ammonia have been emphasized, the potential hepatotoxic effects of ammonia have been less studied. However, there are some reports of histopathological changes in the liver of patients with urea cycle defects. These patients have often repeatedly been exposed to high ammonium levels and this indicates that ammonia may affect the liver as well. ***Aims***: The purpose was to examine how ammonia affects hepatocytes, considering hepatocyte viability, urea production, and expression of selected genes including hepatobiliary transport systems, aquaporins, and nuclear receptors. ***Methods****: In vitro* cell culture of Hep G2 (hepatocellular carcinoma) and H1 cells (human embryonic stem cell line differentiated into derived hepatocyte-like-cells) were used in the experiments. Cell damage and metabolic activity were assessed with aspartate aminotransferase (AST) measurement and MTT assay, respectively. Gene expression analysis was assessed with quantitative RT-PCR, and western blotting was used for protein quantification. Urea production after exposure to ammonium chloride was measured in supernatant in both cell lines. Further, RNA interference (siRNA) experiments were performed to examine whether FXR was involved in regulation of some selected genes. ***Results and conclusion***: We demonstrate that ammonium reduces metabolic activity in Hep G2 cells by MTT assay. In H1 cells ammonium chloride caused increased levels of AST. A dose-dependent increase in urea production after exposure to ammonium chloride was found in both cell lines. Ammonia increased the expression of *AQP8* mRNA. Increased levels of *OATP1* were also found in both cell lines, in addition to increased levels of *AQP9* in Hep G2. After knockdown of *FXR*, *AQP8* was unaffected, indicating that FXR did not have an important role in regulation of *AQP8*. AQP8 protein levels were not increased after exposure to ammonia. Ammonia affects cell damage and metabolic activity in H1 and Hep G2 cells, respectively, and causes changes in expression of some genes in hepatocytes.

Sammendrag

Bakgrunn: Leveren er det viktigste organet med hensyn til å fjerne skadelig ammoniakk, hovedsakelig via urea - og glutamat-glutamin syklusen. Hos pasienter med akutt og kronisk leversvikt opptrer ofte hyperammonemi som en sekundær tilstand. Forhøyet ammoniakkverdier i blodet fører til høyere konsentrasjon av ammoniakk i hjernen, som kan resultere i hepatisk encefalopati og leverkoma. Mens nevrotoksiske effekter av ammoniakk har blitt studert nøye, er effekten av ammoniakk på leveren undersøkt i mindre grad. Imidlertid viser det seg at pasienter med urea syklusdefekter, som blir utsatt for gjentatte episoder med høy ammoniakk, har histopatologiske tegn på forandringer i leveren. ***Mål***: Formålet med denne studien var å undersøke hvordan ammoniakk påvirker hepatocytter med hensyn til levedyktighet, ureaproduksjon og gen ekspresjon av utvalgte gener inkludert hepatobiliære transportsystemer, aquaporiner og kjerne reseptorer. ***Metoder***: *In vitro* cellekultur av Hep G2 (hepatocellulær karsinom), og H1 celler (human embryonale stamcellelinje differensiert til hepatocytt-lignende celler) er benyttet til eksperimentene. Levedyktighet er bestemt med MTT analyse, og celleskade med måling av aspartate aminotransferase (AST). Gen ekspresjons analyser er bestemt ved kvantitativ RT-PCR, og western blott ble benyttet for protein kvantifisering. Ureaproduksjonen etter eksponering for ammoniumklorid ble målt i supernatanten i begge cellelinjer. RNA interferens (siRNA) eksperimenter ble utført for undersøke om FXR regulerte ekspresjon. ***Resultater og konklusjon***: Vi viser at den metabolske aktiviteten i Hep G2 celler var redusert etter eksponering av ammoniakk ved MTT måling. Ammoniakk økte AST utskillelse i H1 cellene. En dose-avhengig økning i ureaproduksjon etter eksponering for ammoniumklorid ble funnet i begge cellelinjer, i tillegg til økt ekspresjon av mRNA *AQP8*. Proteinnivået av AQP8 økte ikke. Økt ekspresjon av *OATP1* ble også funnet i begge cellelinjer, i tillegg til økte nivåer av *AQP9* i Hep G2. Nedregulering av *FXR* endret ikke ekspresjon av *AQP8* og indikerer at denne kjernereseptoren ikke er sentral i reguleringen av AQP8. Ammoniakk påvirker celleskade og metabolsk aktivitet i H1 og Hep G2 celler, og fører til endret ekspresjon av noen gener i hepatocytter.

Abbreviations

ALT	Alanine aminotransferase
AQPs	Aquaporins
ASL	Argininosuccinate lyase
ASS-1	Argininosuccinate synthetase
AST	Aspartate aminotransferase
BBB	Blood brain barrier
CBS	Cerebral blood flow
cDNA	Complementary deoxyribonucleic acid
CPS-1	Carbamoylphosphate synthetase
Ct	Cycle threshold
dNTP	Deoxyribose nucleotide triphosphate
FBS	Fetal bovine serum
FXR	Farnesoid X receptor
GAPDH	Glyceraldehyde-3-Phosphate Dehydrogenase
GDH	Glutamate dehydrogenase
GS	Glutamine synthetase
H1	Human embryonic stem cells, derived to hepatocyte-like-cells
HE	Hepatic encephalopathy
Hep G2	Human hepatocellular carcinoma cells
HRP	Horse radish peroxidase
LD50	Lethal dose 50%
mRNA	Messenger RNA
MRP4	Multidrug resistance protein 4
MTT	3-(4,5-Dimethylthiazol-2-yl)-2,5-Diphenyltetrazolium Bromide
NAGS	N-acetylglutamate synthase
NH_3	Non-ionized ammonia
NH_4^+	Ammonium ions
OATP1	Organic anion-transporting polypeptide 1
ORNT	Ornithine transporter
OTC	Ornithine transcarbamylase
PAG	Phosphate activated glutaminase
PBS	Phosphate buffered saline
Pen/Strep	Penicillin/streptomycin
PXR	Pregnane X receptor
qRT-PCR	Quantitative real-time polymerase chain reaction
Rh	Rhesus
RNA	Ribonucleic acid
RPMI-1640	Roswell Park Memorial Institute medium
SDS	Sodium dodecyl sulphate
SDS-PHAGE	Sodium dodecyl Sulphate polyacrylamide gel
siRNA	Small interfering RNA
TBS-T	Tris-Buffered Saline containing Tween
UCD	Urea cycle defects

Contents

Chapter 1

Introduction

1.1. Ammonia

Nitrogen metabolism is important for cell structure and energy production in normal health. The liver is an essential organ for removing waste products and toxins from your body, including ammonia. In patients with acute and chronic liver failure accumulation of ammonia due to hepatic dysfunction often causes hyperammonemia, which is considered to play a role in the development of hepatic encephalopathy and hepatic coma (Wright et al. 2011). The potential hepatotoxic effects of elevated ammonia levels are less known.

Ammonia exists in two forms, non-ionized (NH_3), and in charged form as ions (NH_4^+). The relationship between ammonia and ammonium ions is reversible: $NH_3 + H^+ \leftrightarrow NH_4^+$. The balance is pH dependent, at pH 9.3 they are in equilibrium (the reaction pKa value), at physiological pH (pH 7.4) 98 % will be present as NH_4^+ (Adeva et al. 2012). For both NH_4^+/NH_3 the term ammonia is used, unless otherwise stated.

1.2. Ammonia metabolism in healthy human

Normally the plasma concentrations of ammonia range from 10 – 40 μmol/L (Wright et al. 2011). Plasma values > 50 μmol/L are defined as hyperammonemia (Haberle 2013). The liver is the main site in ammonia metabolism, where urea cycle, in periportal hepatocytes, and the glutamine-glutamate cycle in perivenous hepatocytes are main pathways for ammonia detoxification through a number of reactions and their key enzymes (Wright et al. 2011). Intestine, kidney, brain, skeletal muscles, skin, lung, and erythrocytes also contribute to regulation of ammonia in the body (Adeva et al. 2012).

1.2.1. Urea cycle

Hepatocytes make use of mainly two products of metabolism, ammonia and carbon dioxide, to generate urea trough a number of reactions called urea cycle (Adeva et al. 2012). The main function of urea cycle is to transform ammonia, from different irreversible oxidative deamination reactions, to the less toxic product urea. Urea is subsequently excreted in the kidneys (Wright et al. 2011). In figure 1.1. the reactions are shown schematically. As summarized by Adeva et al. N-acetylglutamate synthase (NAGS), an enzyme located in mitochondria, produces N-acetylglutamate from glutamate and acetyl-CoA. Initiation of urea cycle requires N-acetylglutamate, an allosteric cofactor. This activates carbamoylphosphate synthetase (CPS-1), an enzyme synthesizing carbamoyl phosphate from ammonia and bicarbonate (and 2 molecules ATP). Carbamoyl phosphate and ornithine are converted to citrulline by the mitochondrial enzyme ornithine transcarbamylase (OTC). Citrulline exits the mitochondria and, together with aspartate, and ATP, is transformed to arginosuccinate by the cytosolic enzyme argininosuccinate synthetase (ASS-1), and further to l-arginine and fumarate by argininosuccinate lyase (ASL). Aspartate is provided by a reaction catalyzed by asparaginase from asparagine, and aspartate passes the mitochondrial membrane through an aspartate-glutamate carrier citrin. Arginase catalyzes arginine to ornithine, and produces urea. Ornithine passes to mitochondria by mitochondrial ornithine transporter (ORNT), completing the cycle (Adeva et al. 2012).

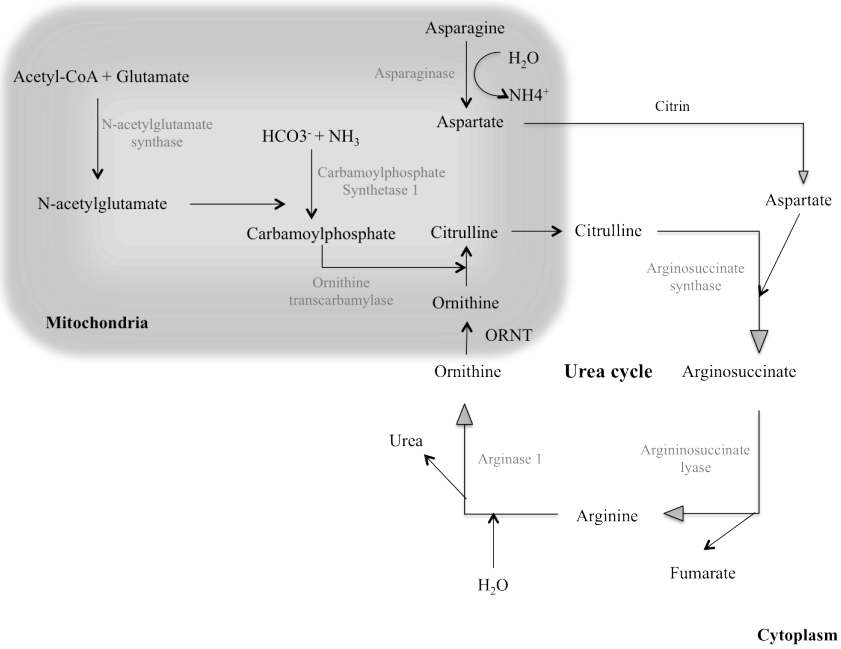

Figure 1.1. Schematic overview of urea cycle (modified from Adeva et al. 2012).

1.2.2. Glutamate – glutamine cycle

Glutamate-glutamine cycle is important for ammonia metabolism in the body through different key enzymes including glutaminase, glutamine synthetase (GS), and glutamate dehydrogenase (GDH). Glutamate and glutamine have important roles in transporting excess ammonia through hepatic ureagenesis (detoxification) or urinary excretion, which both regulates the body's nitrogen balance by maintaining acid-base homeostasis (Nissim 1999). Both glutaminase and glutamate dehydrogenase are located in mitochondria. Glutaminase, phosphate activated (PAG), catalyses the reaction of glutamine to glutamate and free ammonium ions, and GDH catalyses a reversible oxidative deamination reaction, producing free ammonium ions and α-ketoglutarate from glutamate. The reaction uses a cofactor, NAD^+, which releases H^+ and NADH. GS is a cytosolic enzyme producing glutamine from glutamate and ammonium ions (Figure 1.2.) (Adeva et al. 2012).

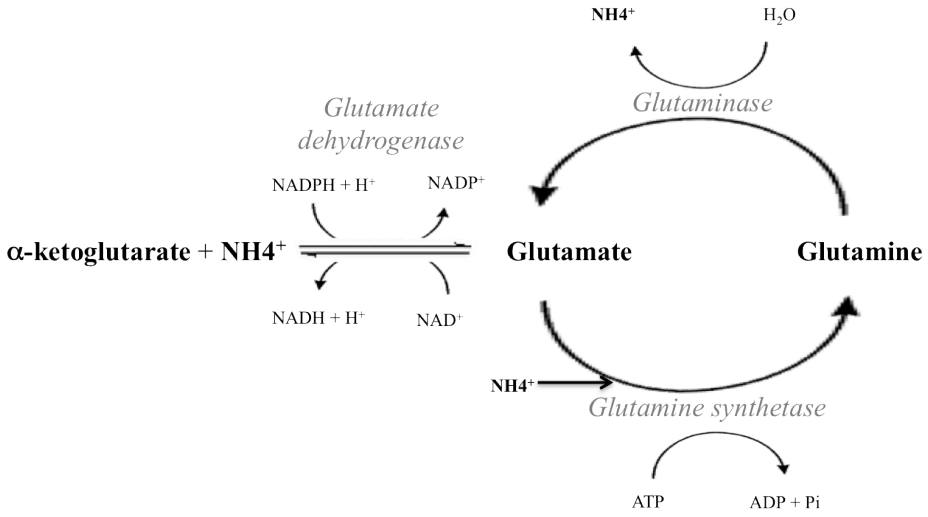

Figure 1.2. Glutamate-glutamine cycle (modified from Adeva et al. 2012).

1.2.3. Ammonia metabolism in other organs

Intestines

The human gastrointestinal tract is both glutamine consuming and ammonia producing organ. Ammonia is formed in the intestine of various reasons: through high protein diet, intestinal bacterial production, and from amino acids formation (Wright et al. 2011). Equal amounts of ammonia are produced in the intestine and the colon in the post-absorptive phase. Ammonia production in the colon is due primarily to bacterial

degradation and urea breakdown (Olde Damink et al. 2002). In the small bowel, where glutaminase is the main enzyme catabolizing glutamine (Romero-Gomez et al. 2004), ammonia production is mainly due to degradation of amino acids (Wright et al. 2011).

Kidney

Excretion of ammonia is carefully regulated through various mechanisms such as tubular urine flow, acid-base balance, and ion exchangers (Wright et al. 2011). The main source of ammonia production in the kidneys is glutamine. During the formation of ammonia, bicarbonate is produced. Ammonia is secreted from proximal tubule cells via Na^+ / H^+ exchanger to lumen, and further reabsorbed in Henle's loop, and transported to the collecting duct (Kim 2009). Approximately 50% of the ammonia produced by the kidneys is excreted through the urine, and the rest to renal vein, under normal circumstances. Ammonium ions in renal veins are an important source of the normal concentration of ammonia in blood (Adeva et al. 2012).

Muscle

Glutamine is necessary for transport of excess ammonia as mention earlier. Skeletal muscle is a major organ in producing glutamine, due to the high mass, although its activity of glutamine synthetase under normal conditions is low (Olde Damink et al. 2009), and neither uptake nor release of ammonia contribute significantly in healthy humans when muscles are resting (Adeva et al. 2012). When hepatic failure occurs other organs need to readjust to high amount of ammonia, and glutamine synthesis in skeletal muscles is an important alternative route for ammonia detoxification (Olde Damink et al. 2009). Skeletal muscle eliminates nitrogen and gains energy through the glucose-alanine cycle. Pyruvate is converted from glucose in muscle, and catabolized to alanine, by alanine transaminase, which further is transferred to the liver. Alanine is converted to ammonia, and pyruvate is regenerated by alanine transaminase and used for glycogenesis (Wright et al. 2011).

Brain

Brain cells contain both glutamine and glutamine synthetase. Glutamine synthetase (GS) is mainly demonstrated in astrocytes, and glutamine in neurones (Olde Damink et al. 2009). At physiological pH, ammonia is mostly present in the blood as NH_4^+. The blood brain barrier is permeable for the non-ionized form, NH_3, through diffusion, but

not for the ionic form, NH_4^+, and thus only small amount of ammonia passes the blood brain barrier under normal conditions (Goldbecker et al. 2010). Glutamine synthetase uses ammonia to produce glutamine that subsequently is transferred to neurons to generate glutamate, and other neurotransmitters. The brain is an important organ for utilization and detoxification of ammonia (Wright et al. 2011), but in healthy humans the net uptake, and release of ammonia seems insignificant (Adeva et al. 2012).

Lung, heart and erythrocytes

Glutaminase synthetase, and phosphate-activated glutaminase are expressed both in lung, and heart, but the roles of these organs in metabolism of ammonia are unclear (Adeva et al. 2012;Wright et al. 2011). Erythrocytes contain Rh proteins, which are described as ammonia transporters, but clinical relevance is uncertain (Adeva et al. 2012).

1.2.4. Ammonia transport and aquaporins

NH_4^+ is transported in the liver by a transport system, Rh glycoproteins. Rh B glycoprotein, and Rh C glycoprotein are located in the liver and in the kidneys. In the liver Rh C is located in bile duct epithelium, where it is believed to be of importance of ammonia secretion in the bile fluid. Rh B is expressed on the basolateral side, proposing that the localization is in the perivenous and not periportal hepatocytes (Weiner & Verlander 2010).

Aquaporins (AQPs) are ubiquitous intrinsic water channels proteins, where the main function is to facilitate water across membranes to maintain homeostasis. In hepatocytes AQP0, AQP8, AQP9 and AQP11 are expressed (Carreras et al. 2007;Rojek et al. 2013). AQP8 is located in the canalicular membrane in hepatocytes, in the mitochondrial membrane, and in intracellular vesicles. Choleretic stimuli, e.g. glucagon can induce trafficking from the vesicles to canalicular membrane (Carreras et al. 2007;Soria et al. 2013). In addition to water, AQP8 is permeable to ammonia. AQP9 is located on the basolateral side in hepatocytes, and is permeable to water, ammonia, glycerol, and urea (Geyer et al. 2013). The functions of intracellular AQP0, and AQP11 are less known (Carreras et al. 2007;Rojek et al. 2013). Holm et al. suggested that NH_3 diffuses over cell membranes through aquaporins (Holm et al. 2005). The mechanisms underlying ammonia transport via aquaporins are not fully understood, but four different

hypotheses are suggested in terms of electrical properties: 1) Ammonia enters through the aquaporin as NH_3. 2) NH_3 enters the aquaporin in addition to H^+, whereas the latter enters in a separate pathway. 3) Both NH3 and H^+ enter the aquaporin. 4) Ammonia enters the aquaporin as NH_4^+ (Litman et al. 2009).

1.3. Hyperammonemia

Hyperammonemia, plasma ammonia > 50 μmol/L, is a metabolic disturbance of excess ammonia, and can be divided in two main groups: primary and secondary. The causes of hyperammonemia can be congenital, genetic defect leading to insufficient urea production, or acquired, due to liver failure. Both types can lead to hepatic encephalopathy, and hepatic coma at a late stage. A third group is increased production of ammonia (Haberle 2013).

1.3.1. Primary hyperammonemia

Primary hyperammonemia is due to inborn error of metabolism. Defect in genes encoding for enzymes, and transporters in the urea cycle, in addition to N-acetylglutamate, which activates the cycle (Haberle 2013). Urea cycle defects (UCD) like deficiency of carbamoylphosphate synthetase, ornithine transcarbamylase, arginosuccinate synthase, arginosuccinate lyase, and arginase are disorders that can lead to critical hyperammonemia (Adeva et al. 2012). The same applies for N-acetylglutamate synthase, where the product is an allosteric activator for carbamoylphosphate synthetase. Defects in genes encoding for the two transporters citrin, and mitochondrial ornithine transporter also lead to hyperammonemia. All UCDs, apart from ornithine transcarbamylase which is inherited X linked, are passed-down in an autosomal recessive pattern (Haberle 2013).

1.3.2. Secondary hyperammonemia

Secondary hyperammonemia is due to inborn errors of intermediary metabolism, inhibition or insufficiency in enzymes that affect the urea cycle. Inhibition of N-acetylglutamate synthetase is suggested to be the mechanism behind hyperammonemia due to metylmalonic aciduria, isovaleric aciduria, and propionic aciduria. Metylmalonic aciduria is due to deficiency or loss in activity of the enzyme methylmalonyl CoA

mutase, and isovaleric aciduria is due to deficiency of isovaleryl CoA dehydrogenase, both are suggested to inhib N-acetylglutamate synthetase (Haberle 2013).
Propionic aciduria is a disorder caused by propionyl CoA carboxylase deficiency, an enzyme catalysing propionyl CoA to methylmalonyl CoA. Hyperammonemia due to propionic aciduria is caused by accumulation of propionyl CoA, which inhibits N-acetylglutamate synthetase, resulting in a non-functional hepatic urea cycle (Abacan & Boneh 2013). Impaired function of the urea cycle can cause hyperammonemia and cerebral edema. Lack of acetyl CoA from carbamoylphosphate synthetase is suggested to be the reason for fatty acid oxidation, and carnitine cycle defects, and lack of substrate in substrate deficiencies to develop hyperammonemia (Haberle 2013).

1.3.3. Drug-associated hyperammonemia

In addition to primary and secondary hyperammonemia other factors can lead to production of ammonia. L-asparginase, mainly used as chemotherapy to treat lymphoblastic leukemia, produces aspartate and ammonia from asparagine (Goodsell 2005). Increased ammonia also occurs due to bacterial overgrowth in the intestine, and following infections in the urinary tract, by higher level of urease. Amino acid infusion as a part of parenteral nutrition also provides increased ammonia (Haberle 2013). The anti-epileptic drug valproate may cause hyperammonemia and in some unusual cases hyperammonemic encephalopathy. Valproyl-CoA, a metabolite produced by valproic acid has an inhibitory effect on N-acetylglutamate synthase, leading to less urea production, and accumulation of ammonia. Other causes are portosystemic shunting, a condition where ammonia bypasses the liver and goes directly into systemic circulation, and glutamine synthetase defects (Haberle 2013).

1.3.4. Liver disease and hyperammonemia

Hepatocellular dysfunction or liver disease can give a rise in plasma ammonia levels. Hyperammonemia occurs as a result of congenital, metabolic or hepatic diseases, and acquired disorders, acute and chronic liver failure (Haberle 2013). Impaired clearance of ammonia from the portal vein through periportal urea cycle and perivenous glutamine synthesis increases the ammonia level. Increased hepatic damage increases the hyperammonemia (Adeva et al. 2012). In an early state of liver failure the detoxification capacity of ammonia in hepatocytes is usually sufficient, but in advanced liver failure,

cirrhosis, the ability to ammonia removal decreases. Another factor that increases levels of ammonia in patients with liver failure is portosystemic shunting. Ammonia goes directly into systemic circulation from the portal system and accumulates as bypass of the liver reduces detoxification (Wright et al. 2011). Further, other factors as gastrointestinal bleeding, infections and acid-base disturbances in patients with liver failure cause increased ammonia level. In addition administration of different drugs may contribute to hyperammonemia (Adeva et al. 2012). Regarding ammonia homeostasis in liver failure other organs play a key role. Skeletal muscles contribute to ammonia clearance in liver failure by increased uptake from the blood to produce glutamine. The kidneys can both produce and excrete ammonia, and acts like a switch (Scott et al. 2013). At the stage before severe hyperammonemia, the kidneys compensate the ammonia metabolism in liver failure by decreasing the release of ammonia to the renal vein, and by increasing glutamine production and excretion. In cirrhosis the expression of phosphate activated glutaminase increases in the intestine, and may be a therapeutic target in hepatic encephalopathy (HE) (Wright et al. 2011).

1.4. Hepatic encephalopathy

1.4.1. Pathogenesis of hepatic encephalopathy

Due to liver failure, both acute and chronic, hepatic encephalopathy (HE) may occur. HE can be classified in four stages (Ferenci et al. 2002):

1. Reduced consciousness, anxiety, decreased performance, and confused attention.
2. Apathy, disorientation, personality change, and inappropriate behaviour.
3. Sleepiness, and higher degree of disorientation. The patient is responsive to verbal stimulis.
4. Coma.

Ammonia seems to play an important role in the development of HE, but in patients with liver failure the levels of plasma ammonia varies, and there has not been a consistent relationship between ammonia levels and the development of HE and hepatic coma. Some patients develop HE with relatively low values, whereas others can withstand much higher values over time (Adeva et al. 2012). In cirrhosis, HE normally develops slowly, due to increased arterial ammonia level of different reasons: portal

systemic shunting, gastrointestinal bleeding, and reduced cycle activity, from both urea and glutamine-glutamate. In acute liver failure the development is rapid and HE and hepatic coma can occur after a few hours or days. The condition can be reversible, due to liver transplant or other treatments, but may also cause severe cerebral damage and sometimes lead to herniation and death (Felipo & Butterworth 2002). Circulating ammonia in the blood enters the brain mainly via diffusion over the blood brain barrier (BBB). At physiological pH (7.4) more frequent as NH_3, but also as NH_4^+, which also indicates that the diffusion of ammonia in the brain is pH dependent.

The urea synthesis is absent in the brain due to lack of two key enzymes: ornithine transcarbamylase and carbamoyl phosphate synthase I. Due to deficiency of urea cycle, excess ammonia is mainly excreted by glutamate-glutamine cycle, both under healthy conditions and under hyperammonemia. Astrocytes consume NH_4^+ from the blood, and glutamine synthetase catalyzes the formation of glutamine from glutamate, which is transferred to presynaptic neurons. Glutamine is converted to glutamate by glutaminase, and released to synaptic cleft. Glutamate acts either on receptors in postsynaptic neurons or, via glutamate transporters, and is transferred back to astrocytes. In hyperammonemia the expression of these receptors are reduced and the concentration of extracellular glutamate increases (Felipo & Butterworth 2002). Both astrocyte morphology, and some key proteins change due to hyperammonemia. Glutamine synthetase, an enzyme located in astrocytes, catabolizes ammonia and glutamate to glutamine. Glutamine regulates osmotic balance by transporting water into the cell, and accumulation of glutamine may lead to astrocyte swelling and edema (Cichoz-Lach & Michalak 2013). Water enters the brain by diffusion or by water channels (aquaporins) where AQP4 is the dominant, over the BBB. The mechanism of astrocyte swelling, due to ammonia is still to be fully understood, but increased ammonia uptake disrupts cells function, and the concentration of circulating ammonia has been shown to correspond with edema (Scott et al. 2013). Edema is also associated with increased cerebral blood flow (CBF) in acute liver failure at the late stages of HE (Felipo & Butterworth 2002). Oxidative stress, the glutamate/GABA-glutamine cycle, and dysfunction in the BBB are other factors that play a role in HE (Ciecko-Michalska et al. 2012)

1.4.2. Treatment

Liver dialysis

For patients facing liver diseases or liver failure a transplant may be necessary to survive. However, in the acute situation a suitable organ may not be available in time. To expand the time-window and to limit the damage caused by hepatic encephalopathy several stratigies have been suggested. Albumin dialysis is an important tool for removal of toxic substances in the body. Several devices have been tested. Molecular Adsorbent Recirculation System (MARS) is based on albumin, and remove both water-soluble and toxins bounded to proteins, by regenerating albumin, and increased binding capacity. In addition it appears to be an important tool in treatment of hemodynamic instability and hepatic encephalopathy among others, complications due to liver failure (Mitzner 2011).

Pharmacology treatment

Arginine is used in treatment of argininosuccinate lyase deficiency as a supplement to reduced oral protein intake, in addition to intravenous lipids and glucose (Nagamani et al. 2012). Carbaglu is used in treatment of hyperammonemia due to N-acetylglutamate synthase deficiency or carbamoylphosphate synthetase deficiency. Carbaglu works as a synthetic analog of N-acetylglutamate, necessary for the urea cycle to function (Lazier et al. 2014). Carbaglu is also used to treat hyperammonemia due to propionic acidaemia, deficiency of propionyl-CoA carboxylase, where N-acetylglutamate synthase is inhibited due to accumulation of propionyl-CoA (Abacan & Boneh 2013), and there are case reports on the effect of carbaglu of hyperammmonemia associated with valproate (Matoori & Leroux 2015). Sodium benzoate and sodium phenylbutyrate are used in treatment for ornithine transcarbamylase deficiency. Phenylbutyrate binds to glutamine forming phenylacetyl-glutamine (Maestri et al. 1996), and benzoate is thought to activate an alternative pathway for ammonia detoxification by conjugation to glycine forming hippuric acid, both excreted in the kidneys (Misel et al. 2013). Further lactuloses is believed to produce lactic acid and acetic acid, leading to reduced pH, and inhibition of ammonia producing bacteria in the intestine, hence lactulose is used in treatment of hepatic encephalopathy. Different types of antibiotics, such as rifaximin, neomycin, metronidazole, and nitazoxanide, are used to reduce ammonia production in the intestines, due to urease producing bacteria (Al Sibae & McGuire 2009).

1.4.3. Liver changes in urea cycle defects

While ammonia has an important role in hepatic encephalopathy the possible effects of ammonia on the liver have been less studied. Damage in the liver has been demonstrated in patients with urea cycle defects (UCDs). Yaplito-Lee et al. studied histopathological changes in patients with known UCDs. 13 patients, seven with deficiency of ornithine transcarbamylase (OTC), three with carbamoyl phosphate synthetase 1 (CPS1), two with argininosuccinate lyase (ASL), and one with argininosuccinate aynthetase (ASS) deficiency were included in their study. When these patients were diagnosed, the ammonia levels ranged from 168 to 2334 μmol/L. Samples were obtained from liver biopsies both before and after liver transplantation, and post-mortem. Normal to non-specific changes and increased glycogen were found in patients with OTC deficiency. In CPS1 deficiency no changes was found except from moderate fatty change. Cholestasis where found in ASS deficiency, and increased glycogen, moderate fatty change, fibrosis and enlarged pale hepatocytes were found in ASL. A low number of patients and high mortality rate makes the study of long-term consequences of hepatocyte changes in UCDs difficult (Yaplito-Lee et al. 2013). In addition to Yaplito-Lee et al. several case reports have shown histopathological liver changes in patients UCDs. Increased glycogen is reported in OTC, ASL, CPS1, and ASS deficiencies. ASL and ASS have shown diffuse swelling of hepatocytes. Cholestasis, variable fibrosis, and steatosis are found in patients with OTC and ASS deficiencies. There are also reported variable changes in mitochondria in OTC and CPS1, fibrosis in patients with ASL, ASS, CPS1 and OTC, necrosis in OTC, and cirrhosis in ASL deficient patients (Badizadegan & Perez-Atayde 1997;Capistrano-Estrada et al. 1994;LaBrecque et al. 1979;Miles et al. 2005;Mori et al. 2002;Zimmermann et al. 1986).

1.5. Aim of study

Hyperammonemia, a metabolic condition, occurs in patients with hepatocellular dysfunction and becomes neurotoxic. Elevated levels of ammonia can lead to development of hepatic encephalopathy and hepatic coma. The effects of ammonia on the liver and hepatocytes itself are less known.

The main goal of this study was to examine the effects of ammonia on cultivated hepatocytes.

1. Does ammonia change hepatocyte viability?
2. Does ammonia affect urea production in hepatocytes?
3. Does ammonia change gene expression of selected genes in hepatocytes?

Chapter 2

Materials and Methods

2.1. Cells and culturing

2.1.1. Cell line

Hep G2 (HB-8065™) cells were obtained from ATCC® (US). These epithelial liver cells originate from a hepatocellular carcinoma obtained from a 15-year-old Caucasian male.

2.1.2. Cell culturing

Frozen Hep G2 cells from ATCC® were cultured following manufacturer instructions. Cultivation was performed in an aseptic environment. Adherent Hep G2 cells were cultured in complete growth medium; Roswell Park Memorial Institute medium (RPMI-1640) (Lonza, Belgium) supplemented with 10% Fetal Bovine Serum (FBS) (Lonza, Belgium) of South America Origin, 100 U/mL penicillin, and 100 µg/mL streptomycin (Pen/Strep) (Life Technologies, US). Cells were washed with Phosphate Buffered Saline (PBS) (Lonza, Belgium), and detached by adding 3 mL 0.25% Trypsin- Etylen-Diamin-Tetra-Acetat (EDTA-Trypsin) (Lonza, Belgium). After incubation, 10 minutes at 37°C, 5 mL RPMI-1640 was added and the cell suspension was transferred to 15 mL tubes (Sarstedt, Germany), and centrifuged for 3 minutes at 252g. Supernatant was discarded; cells were resuspended in complete growth medium, and plated in 75 cm^2 Nunc™ Cell Culture Treated EasYFlasks™ (Thermo Fisher Scientific, Denmark). Cells

were incubated in a humidified atmosphere at 37°C with 5% CO_2. Medium was changed twice per week and passages used for the experiments ranged from 3 to 15.

2.1.3. Treatment of Hep G2 cells

Hep G2 cells in complete growth medium were diluted 1:10 with 0.4% trypan blue solution (Sigma-Aldrich, US) and further counted under a light microscope (Zeiss, Germany) using Bürker counting chamber (0.0025mm^2) to determine cell concentration. 100.000 cells per well were seeded in 12 well plates (Corning Life sciences, US) to a total volume of 1 mL cell suspension/well, and incubated for 24 hours in 37°C with 5% CO_2. All experiments were performed this way unless otherwise stated. Hep G2 cells were further exposed for different concentrations (0.1, 0.5, 1.0, or 10 mmol/L) of Ammonium chloride (VWR International, Belgium), or Ammonium acetate (Sigma, Germany), and incubated at 37°C with 5% CO_2 for 24, 48, or 72 hours. Total RNA was isolated (chapter 2.3.1.) after 24 or 48 hours. The effects of rutin (100 µmol/L) (Sigma-Aldrich, US) and carglumic acid (100 µmol/L) (Sigma-Aldrich, US) on ammonia toxicity were also tested. Proteins exposed to ammonium chloride were isolated (chapter 2.4.1.) after 72 hours. MTT was measured after 24 or 48 hours (chapter 2.2.1.).

2.1.4. Transfection of small interfering RNA against *FXR* and *AQP8* in Hep G2 cells

Small interfering RNA NR1H4 (*FXR*) (ID: s19373, cat# 4392420) was diluted in Opti-MEM® I (Life Technologies, US) to a concentration of 100 nM. 200 µL of this solution was added along with 2 µL Lipofectamine® RNAiMAX (Invitrogen, US) to each well in 12 wells plates. 100.000 cells per well in RPMI-1640 supplemented with 10% FBS (no Pen/Strep added), were added to a final volume of 1 mL per well after 20 minutes. The cells were incubated for 48 hours at 37°C with 5% CO_2. After 48 hours 10 mmol/L ammonium chloride was added, and incubated for 24 hours at 37°C with 5% CO_2. The same procedure was used for small interfering RNA *AQP8* (ID: s1485, cat# 4392420). Final concentration of siRNA (both for *FXR* and *AQP8*) was 20 nmol/L. Total RNA was isolated (chapter 2.3.1.) after 48 and 72 hours for *FXR*, and 72 hours for *AQP8*.

2.1.5. Human embryonic stem cell line - H1

Dr. Gareth Sullivan and Richard Siller at Institute of Basic Medical Sciences, University of Oslo, kindly provided stem cells for experiments with ammonium chloride. Human embryonic stem cell line H1 was differentiated into small molecule derived hepatocyte-like-cells (H1) with a protocol established in their laboratory (Siller et al. 2015). H1 cells were seeded on 6 wells plate (~ 440 000 cells per well), and exposed to 0.5, and 10 mmol/L ammonium chloride. Medium was refreshed every 24 hours. RNA (chapter 2.3.1.), and protein (chapter 2.4.1.) were isolated after 48 and 72 hours, respectively.

2.2. Cell viability

2.2.1. Cell proliferation by MTT assay

Metabolic activity in Hep G2 was evaluated by 3-(4,5-Dimethylthiazol-2-yl)-2,5-Diphenyltetrazolium Bromide (MTT) (Sigma-Aldrich, US) method (Mosmann 1983). MTT was dissolved in PBS to a concentration of 0.5 mg/mL, and Glucose (Sigma-Aldrich, US) was added to a concentration of 550 µM. Hep G2 cells were exposed to different concentrations of ammonium chloride, or ammonium acetate for 24, and 48 hours (Chapter 2.1.3.), and then 500 µL MTT solution was added, and incubated for 60 minutes at 37°C with 5% CO_2. After incubation the MTT solution was removed and discarded and 500 µL Dimethyl sulfoxide (Sigma-Aldrich, US) was added to each well. The formazan product dissolved in the DMSO solution, and after 15 minutes at ambient temperature 200 µL of each sample was transferred to a microtiter plate (Greiner Bio-One, Germany), and measured photometrically at a wavelength of 570 nm using Multiskan Ascent and Ascent software (Thermo Electron Corporation, US). OD at 690 nm was subtracted. OD was related to controls in each plate.

2.3. Gene expression techniques

2.3.1. Isolation of total RNA

Total RNA was isolated using E.Z.N.A.® Total RNA Kit I (Omega, US). Cells were washed with PBS and lysed with TKR lysis buffer containing 2% β-mercaptoethanol.

The lysed cells were mixed with 70% ethanol, and the samples were placed in HiBIND® RNA mini columns followed by two washing steps with RNA Wash Buffer I. 75 µL of E.Z.N.A Dnase I Digestion buffer containing 2% Rnase-free Dnase I was added and samples were incubated for 15 minutes at ambient temperature. Cells were washed with RNA Wash Buffer I and further twice with RNA Wash Buffer II. 40 µL DEPC water was added to each columns, and the samples were centrifuged and stored in -70°C. Amount and purity of RNA was measured using NanoDrop ND-1000 (Saveen Werner, Sweden).

2.3.2. cDNA synthesis

cDNA was synthesised from mRNA using High-Capacity cDNA Reverse Transcription Kit (Applied Biosystems, US). RNA samples were diluted in nuclease-free H_2O (Life technologies, US), and master mix (42% 10xRT buffer, 8% dNTP, 20% random primers and 10% Multiscribe Reverse transcriptase) was added to a total amount of 50 ng/µL. For single interfering RNA (chapter 2.1.4.) and H1 cells (chapter 2.1.5.) experiments, the final cDNA concentrations were 25 ng/µL. Revers transcription was performed in a thermal cycler (PTC-100™) (US). See table 2.1. for program conditions.

Table 2.1. Program for cDNA synthesis

	Step 1	**Step 2**	**Step 3**	**Step 4**
Temperature	25°C	37°C	85°C	4°C
Time (minutes)	10	120	5	∞
Process	Annealing	Reverse transcription	Enzyme denaturation	Final extension

2.3.3. Quantitative RT-PCR for mRNA expression

Total RNA was extracted after different time points (chapter 2.1.3., and 2.3.1.) and reverse transcribed to cDNA (chapter 2.3.2.). Glyceraldehyde 3-phosphate dehydrogenase (*GAPDH*) was used as endogenous control, and mRNA expression was measured for the human genes farnesoid X receptor (*FXR*), pregnane X receptor (*PXR*), organic anion transporting polypeptide 1 (*OATP1*), multidrug resistance protein 4 (*MRP4*), aquaporin 8 (*AQP8*), and aquaporin 9 (*AQP9*). Primer sequences for the

different genes are shown in table 2.2. Samples were diluted to a total concentration of 10 ng/µL for all experiments. Master mix was prepared for each gene containing 63% Power SYBR® Green (Applied Biosystems, US), and 3% of both forward and reverse primer (10 pmol/µL). Master mix and samples were added to a final concentration of 2 ng/µL sample per PCR reaction. Quantitative Real-Time PCR (qRT-PCR) program used are shown in table 2.3., and carried out with Applied Biosystems® ViiA™ 7 instrument, with 96-well block, comparative Ct experiment, SYBR® green reagent, and standard properties settings (Applied Biosystems, US).

Table 2.2. Primers used in Quantitative Real-Time PCR

Gene	Forward primer (5´- 3´)	Reverse primer (5´- 3´)	Manufacturer
Human *GAPDH*	TCAAGCTCATTTCCTGGTATGACAACGAA	CTCTCTCTTCCTCTTGTGCTCTTGCT	Invitrogen™
Human *FXR*	CCTGTGAGGGGTGTAAAGGTTTC	CCTTAGTCGACACTCTTGACACTTTC	Invitrogen™
Human *PXR*	GGCCACTGGCTATCACTTCAA	TTCATGGCCCTCTTGAAAA	Eurofins MWG Operon
Human *OATP1*	GGGATGACTGTGAATGGCTT	GTAGCTGACGAAGGTGAGGC	Invitrogen™
Human *MRP4*	CTGTGATAGGAGATCGGGGA	CTGAGAGGATCGTCCAGGAG	Invitrogen™
Human *AQP8*	AGGTTCTGGAATGCATCTGG	AGGGCCCTTTGTCTTCTCAT	Invitrogen™
Human *AQP9*	AGCCACCTCTGGTCTTGCTA	GAAGGTGCATCCCTTGATGT	Invitrogen™

Table 2.3. Quantitative Real-Time PCR program

Stage	Step	Temperature	Time (minutes)
Hold stage	1	50 °C	02:00
	2	95 °C	10:00
PCR stage	1	95 °C	00:15
Number of cycles: 40	2	60 °C	01:00
Melt curve stage	1	95 °C	00:15
	2	60 °C	01:00

After qRT-PCR reactions both melting curves (Tm) and threshold cycle (Ct) values were calculate by Applied Biosystems® ViiA™ 7 software (US). The melting curves were used to verify the amplification specificity, and Ct values for calculating relative gene expression using the ΔΔCt method. Target genes were normalized to *GAPDH*, reference gene, and relative gene expression between samples was compared to control sample (untreated cells) by the formula $2^{-(_{\Delta\Delta}Ct)}$.

2.4. Protein expression techniques

2.4.1. Isolation of protein

Hep G2 cells (chapter 2.1.3.) were washed with cold PBS. After discarding PBS, 200 µL EDTA-trypsin was added and incubated for 10 minutes in 37°C with 5% CO_2. Cold RPMI-1640 with 10% FBS was added and cells were transferred to 15 mL tubes and centrifuged for 5 minutes at 252g in 4°C. Supernatants were removed and cell pellets were dissolved in 1 mL cold PBS. H1 cells were washed, and scraped with 1 mL cold PBS. Subsequently cells were transferred to 1.5 mL tubes, and centrifuged for 5 minutes, 1231g, at 4°C. Supernatants were discarded and 25 µL of 1 x cell lysis buffer from Cell Signalling Technology (cat# 9803) were added to each sample, and vortexed. After 30 minutes on ice the cells were centrifuged for 10 minutes, 16060g at 4°C, and the supernatants were placed in new tubes and stored at -20°C.

2.4.2. Protein quantification

BioRad DC™ Protein Assay (cat# 500112) (Bio-Rad, US) was used to quantify protein concentration. Protein standard curve was prepared by diluting Bovine Serum Albumin (BSA) (Sigma-Aldrich, US) in the lysis buffer used for isolation of protein (chapter 2.4.1). The samples were diluted when required. 5 µL of standards or samples were added in duplicates to a 96 wells microtiter plate. 25 µL of a mix containing 20 µL of reagent S (surfactant solution) per 1 mL reagent A (alkaline copper tartrate solution) was added to each well followed by 200 µL of reagent B (Folin reagent). After 15 minutes in room temperature the absorbance was measured photometrically at a wavelength of 690 nm using Multiskan Ascent and Ascent software (Thermo Electron Corporation, US).

2.4.3. Western Blotting

Western blotting was used to detect and quantify AQP8 expression in Hep G2 cells after 48 and 72 hours (chapter 2.1.3.) and in H1 cells after 72 hours (chapter 2.1.5.). Samples were prepared by adjusting volume with Sodium dodecyl sulfate (SDS) lysis buffer, and 2 µL sample buffer to an amount of 20 µg protein in a total volume of 15 µL. The samples were heated for 5 minutes at 95°C. PageRuler™ Plus Prestained

Protein Ladder (10-170 kDa) (Life Technologies, US) was used to determine band size. The proteins were separated by sodium dodecyl sulfate polyacrylamide gel electrophoresis (SDS-PAGE), 45 and 30 minutes at 70 and 100V, respectively, using Mini-PROTEAN® TGX™ precast gel (Bio-Rad, US). Further the proteins were transferred to a nitrocellulose blotting membrane (GE Healthcare, UK) at 100V for 60 minutes. Membranes were blocked with Tris-Buffered Saline with 0.1% Tween 20 (Sigma-Aldrich, US) (TBS-T) containing 5% milk (Bio-Rad, US) for 60 minutes, and washed in TBS-T before incubation with primary antibody diluted in TBS-T with 5% milk over night at 4°C (table.2.4.). After incubation with primary antibody the membranes were washed 3 x 15 minutes in TBS-T. Membranes were then incubated for 60 minutes at ambient temperature with a secondary horseradish peroxidase-coupled anti-mouse/anti-goat-IgG antibody (table 2.4.) diluted in TBS-T with 5% milk. Washing steps (3 x 15 minutes in TBS-T) were performed before ECL™ Prime Western Blotting Detection Reagent (GE Healthcare, UK) was used to visualize bands. Pictures were captured with G:BOX system (Syngene, UK), and data were calculated with GeneTools analysis software (Syngene, UK). All data were normalized to endogenous controls, β-actin (Santa Cruz biotechnology, US).

Table 2.4. Antibodies used in Western Blotting

Primary antibody	**Cat. #**	**Dilution**	**Manufacturer**
AQP8 mouse monoclonal IgG_{2a}	SC-81870	1:100	Santa Cruz Biotechnology, Inc.
Actin goat polyclonal IgG	SC-1616	1:1000	Santa Cruz Biotechnology, Inc.
Secondary antibody			
Goat anti-mouse IgG-HRP	SC-2005	1:1000	Santa Cruz Biotechnology, Inc.
Donkey anti-goat IgG-HRP	SC-2020	1:2000	Santa Cruz Biotechnology, Inc.

2.5. Urea

Urea was measured on Modular Analytical platform P800 (Roche Diagnostics, Germany) by kinetic UV assays (Roche UREA/BUN, cat# 11729691216, Roche diagnostics, Germany) at the Department of Medical Biochemistry, OUS-Rikshospitalet.

2.6. Aspartate aminotransferase

Aspartate aminotransferase (AST) activity was measured on Modular Analytical platform P800 by an enzymatic photometric method (Roche AST (ASAT/GOT), cat# 11876848, Roche diagnostics, Germany) at the Department of Medical Biochemistry, OUS-Rikshospitalet.

2.7. pH

pH was measured with Radiometer PHM 92 Lab pH Meter (Denmark) in RPMI-1640 and RPMI-1640 containing 10 mmol/L ammonium chloride. The medium was heated to 37°C, and gassed with CO_2 for 10 minutes before pH was measured.

2.8. Statistical analysis

Graph Pad Instat version 03.10 for windows and Graph Prism 6.00 for mac (GraphPad® Software Inc, San Diego, California) were used for statistical analyses. Data are reported as means and standard deviations. Comparisons between the two groups were done with unpaired t-tests or unpaired t-test with welch correction. Multiple groups were analysed with one-way ANOVA. Dunnett's post hoc test was used for urea and AST. A two-tailed p-value less than 0.05 was considered significant.

Chapter 3

Results

3.1. Cell viability

3.1.1. Effect of ammonia on hepatocyte viability

Hep G2 cells were incubated with ammonium acetate (figure 3.1.) or ammonium chloride (figure 3.2.) for 24, and 48 hours. Both were associated with a dose dependent decrease in metabolic activity measured by MTT after 24 hours. Extending the incubation time with 10 mM ammonium acetate from 24 to 48 hours lowered the MTT cleavage further from 75 ± 2.6% of controls to 56 ± 3.1% of controls ($p<0.01$, n=3). Ammonium acetate and ammonium chloride demonstrate a similar pattern in terms of viability. Addition of 10 mmol/L ammonium chloride to cell medium (pH 7.34 ± 0.01) did not change pH compared to controls (pH 7.30 ± 0.06) ($p=0.32$, n=3). Incubation of Hep G2 cells with either ammonium acetate (figure 3.3.A.) or ammonium chloride (figure 3.3.B.) for 24 or 48 hours demonstrated loss in cell density. To investigate whether formation of oxygen free radicals could contribute to the damage, Hep G2 cells were incubated with the antioxidant rutin (100 μmol/L) and 10 mmol/L ammonium chloride for 48 hours. Rutin did not significantly change MTT reduction: controls (198 ± 15%, n=10), ammonium chloride (100 ± 1.4%, n=5), ammonium chloride/rutin (104.8 ± 8.7%, n=6) ($p=0.24$). Carglumic acid (100 μmol/L), a structural analogue of N-acetylglutamate, was added to Hep G2 cells exposed to 10 mmol/L ammonium chloride and incubated for 48 hours. Addition of carglumic acid (92 ± 6.9%, n=4) did not significantly improve MTT cleavage ($p=0.10$) compared to ammonium chloride (100 ±

0.4%, n=4), (controls, 173 ± 11%, n=5). This indicates that toxicity by ammonium chloride on Hep G2 cells was not caused by depletion of N-acetylglutamate.

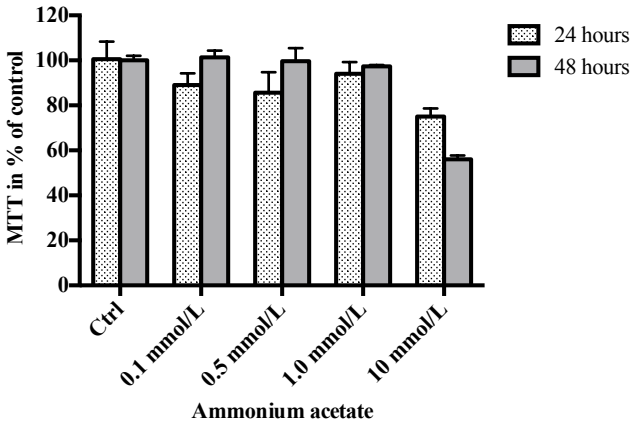

Figure 3.1. **Effect of ammonium acetate on metabolic activity in Hep G2 cells**. Hep G2 cells were exposed to different concentrations of ammonium acetate (0.1, 0.5, 1.0, or 10 mmol/L) for 24, and 48 hours. Cell viability was measured with MTT assay, and the data are presented as % mean and SD (n=3).

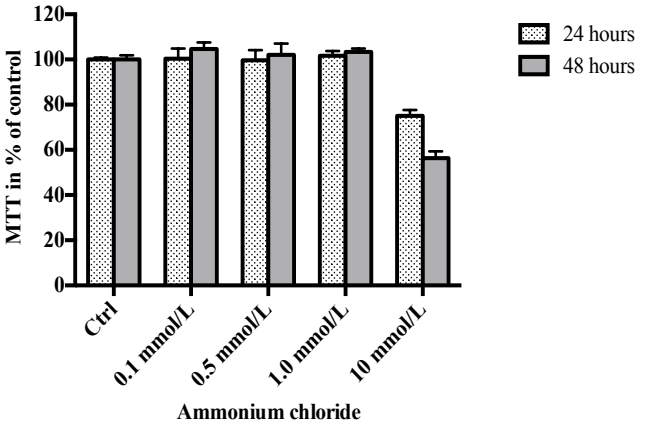

Figure 3.2. **Effect of ammonium chloride on metabolic activity in Hep G2 cells**. Hep G2 cells were exposed to different concentrations of ammonium acetate (0.1, 0.5, 1.0, or 10 mmol/L) for 24, and 48 hours. Cell viability was measured with MTT assay, and the data are presented as % mean and SD (n=3).

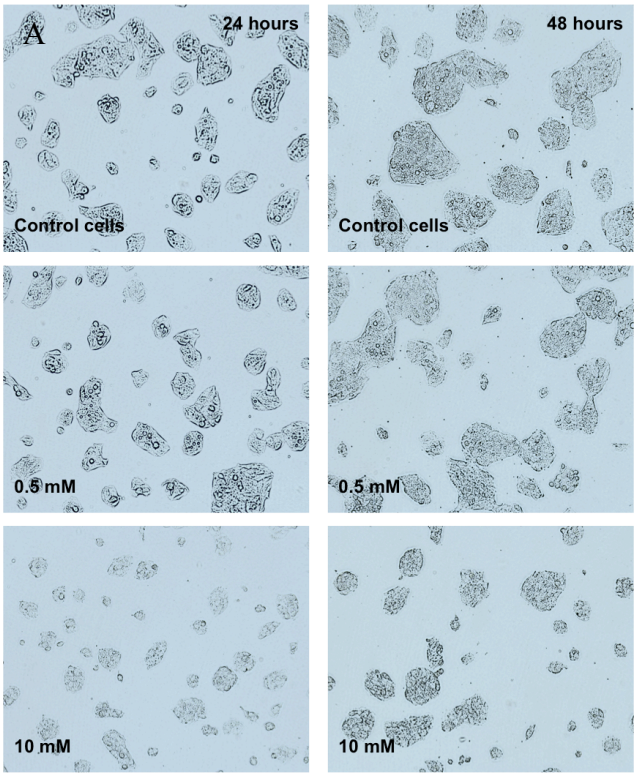

Figure 3.3.A. **Cell morphology after exposure for ammonium acetate**. Hep G2 cells were plated with a density of 100.000 cells per well, passage 4, and exposed to ammonium acetate (0.5 or 10 mmol/L) for 24 or 48 hours.

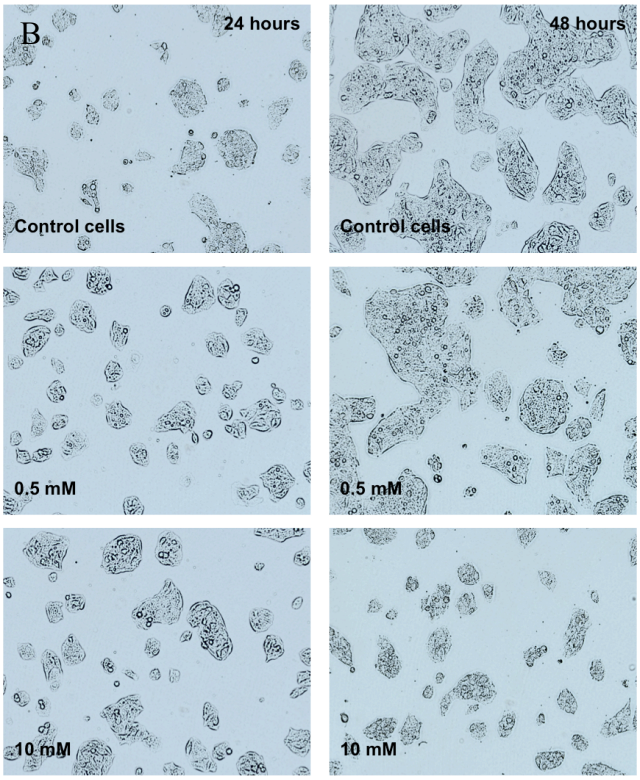

Figure 3.3.B. **Cell morphology after exposure for ammonium chloride**. Hep G2 cells were plated with a density of 100.000 cells per well, passage 4, and exposed to ammonium chloride (0.5 or 10 mmol/L) for 24 or 48 hour.

3.1.2. Aspartate aminotransferase measurement

Aspartate aminotransferase (AST) and alanine aminotransferase (ALT) were measured in supernatant after 48 hours incubation in Hep G2 cells exposed to ammonium chloride, but 100.000 cells per well did just produce enzymes above the threshold for the used methods. The toxicity of ammonium chloride was also measured in another cell line H1, stem cells differentiated into hepatocyte-like-cells, after incubation with 0.5 or 10 mmol/L ammonium chloride for 48 hours. AST level in the supernatant was significantly ($p<0.01$) increased in the cells exposed to 10 mmol/L ammonium chloride (14.0 ± 0.6 U/L, n=3) compared with controls (5.0 ± 0.6 U/L, n=3) (figure 3.4.).

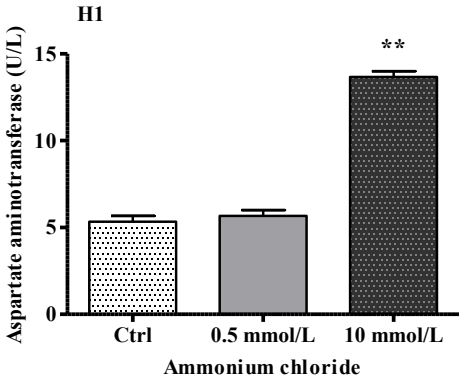

Figure 3.4. **Effect of ammonium chloride on AST release from H1 cells**. AST was measured in supernatants after 48 hours in H1 cells after treatment with 0.5, or 10 mmol/L ammonium chloride. Data are presented as mean and SD (n=3). ** Indicates $p<0.01$.

3.2. Urea production

3.2.1. Effect of ammonia on urea formation

The concentration of urea in the supernatant from Hep G2 cells (control, 1.69 ± 0.09 mmol/L, n=3) was slightly higher than in the culture media (1.06 mmol/L, n=1) indicating a low basal production of urea. Urea was also measured in the supernatant after incubation with 0.5 or 10 mmol/L ammonium chloride for 48 hours in both Hep G2 cells (figure 3.5.) and H1 cells (figure 3.6.). Hep G2 cells exposed to 0.5 mmol/L (1.9 ± 0.13 mmol/L, n=3) of ammonium chloride did not significantly ($p=0.07$) increase urea concentration in the supernatant compared to controls (1.69 ± 0.09 mmol/L, n=3), but in contrast 10 mmol/L ammonium chloride (4.3 ± 0.26 mmol/L, n=3) caused a significant ($p<0.01$) increase in urea concentration. In the H1 cell line a higher urea concentration was found in the supernatant after exposure for 10 mmol/L ammonium chloride for 48 hours (17.76 ± 0.56 mmol/L, n=3) than in controls (0.96 ± 0.04 mmol/L, n=3) ($p<0.01$). Urea was also slightly higher in wells with 0.5 mmol/L ammonium chloride (1.6 ± 0.13) than in controls (0.96 ± 0.04 mmol/L, n=3). Both Hep G2 and H1 dose-dependently increased urea production after exposure to ammonium chloride.

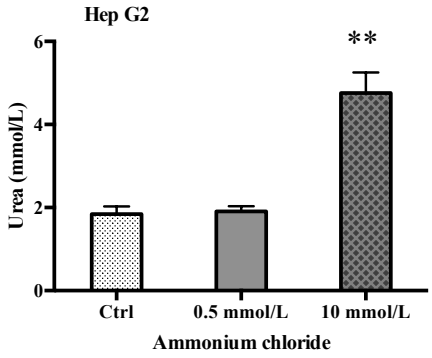

Figure 3.5. **Urea production of Hep G2 cells**. Urea was measured in supernatant after 48 hours in Hep G2 cells after treatment with 0.5, or 10 mmol/L ammonium chloride. Data are presented as mean and SD (n=6 for ctrl, and 10 mmol/L, n=3 for 0.5 mmol/L). ** Indicates $p<0.01$.

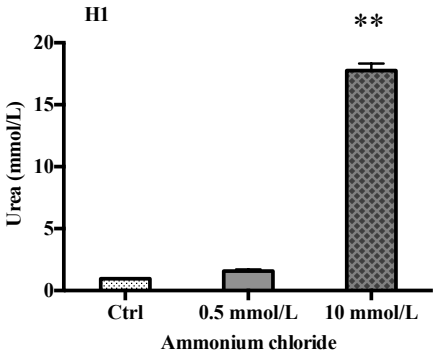

Figure 3.6. **Urea production of H1 cells**. Urea was measured in supernatant after 48 hours in H1 cells after treatment with 0.5, or 10 mmol/L ammonium chloride. Data are presented as mean and SD (n=3). ** Indicates $p<0.01$.

3.3. mRNA expression in the liver after ammonia exposure

3.3.1. Effect of ammonia on hepatocyte gene expression

As demonstrated ammonia causes reduced metabolic activity and increases urea production in hepatocytes. We also wanted to explore the effect of ammonia on gene expression of selected hepatobiliary transport systems (*OATP1, MRP4*), aquaporins (*AQP8, AQP9*), and nuclear receptors (*FXR, PXR*). The effect of ammonia on relative mRNA expression levels both in Hep G2 and H1 cells were assessed with qRT-PCR. Ammonium acetate (figure 3.7.) and ammonium chloride (figure 3.8.) essentially gave similar results in Hep G2 cells. Incubation with ammonium acetate for 24 and 48 hours ($p<0.0001$, n=3), and ammonium chloride for 24 hours ($p<0.05$, n=3) and 48 hours ($p<0.0001$, n=3) both caused a dose-dependent mRNA level increase of *AQP8*. Ammonium acetate increased mRNA expression of *OATP1* ($p<0.01$, n=3) after 24 hours, and *AQP9* ($p<0.01$, n=3) after 48 hours. Ammonium chloride increased expression of *AQP9* ($p<0.001$, n=3) and *FXR* ($p<0.001$, n=3) after 48 hours. Ammonium acetate and ammonium chloride essentially gave similar results and thus only ammonium chloride was used for further experiments. Exposing H1 cell to 10

mmol/L ammonium chloride for 48 hours increased expression of *OATP1* ($p<0.01$), and *FXR* ($p<0.05$) (figure 3.9.).

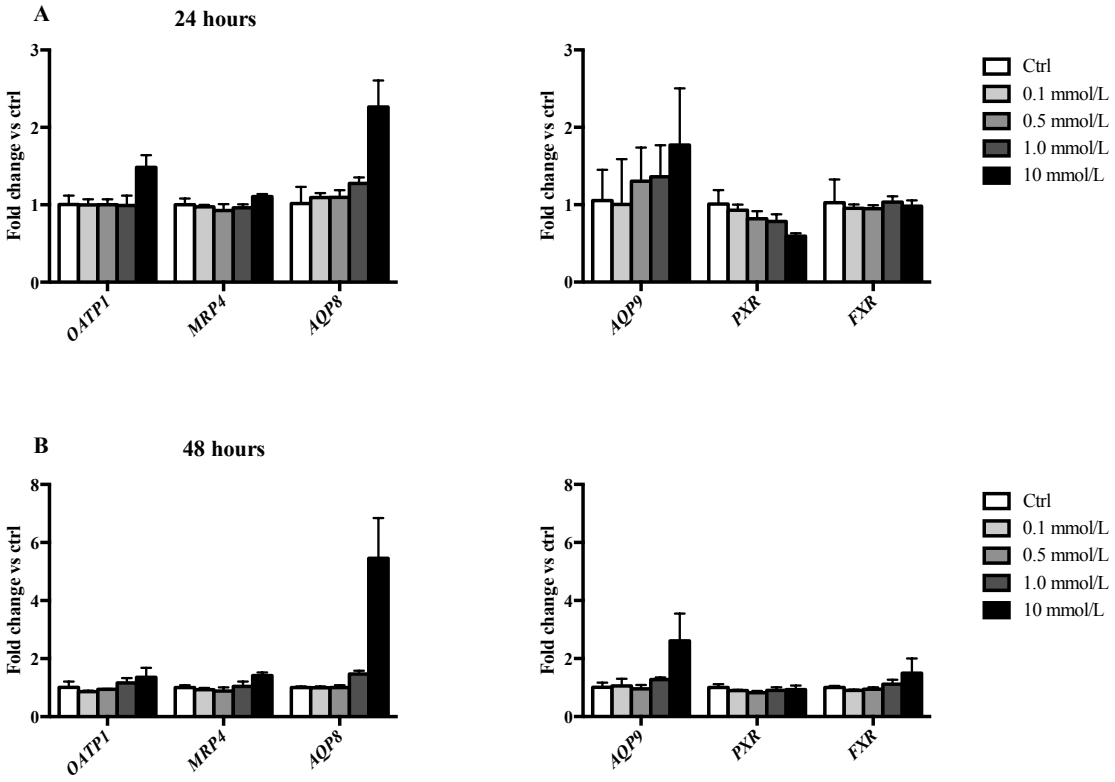

Figure 3.7. **Effect of ammonium acetate on relative mRNA expression level in Hep G2 cells**. The effect of different concentration of ammonium acetate (0.1, 0.5, 1.0, or 10 mmol/L) on relative mRNA expression levels of *OATP1*, *MRP4*, *AQP8*, *AQP9*, *FXR*, and *PXR* in Hep G2 cells (~100.000 cells per well, 12 wells plate, at 37°C with 5% CO_2) were measured after 24 (A), or 48 (B) hours. The data are presented as mean and SD (n=3).

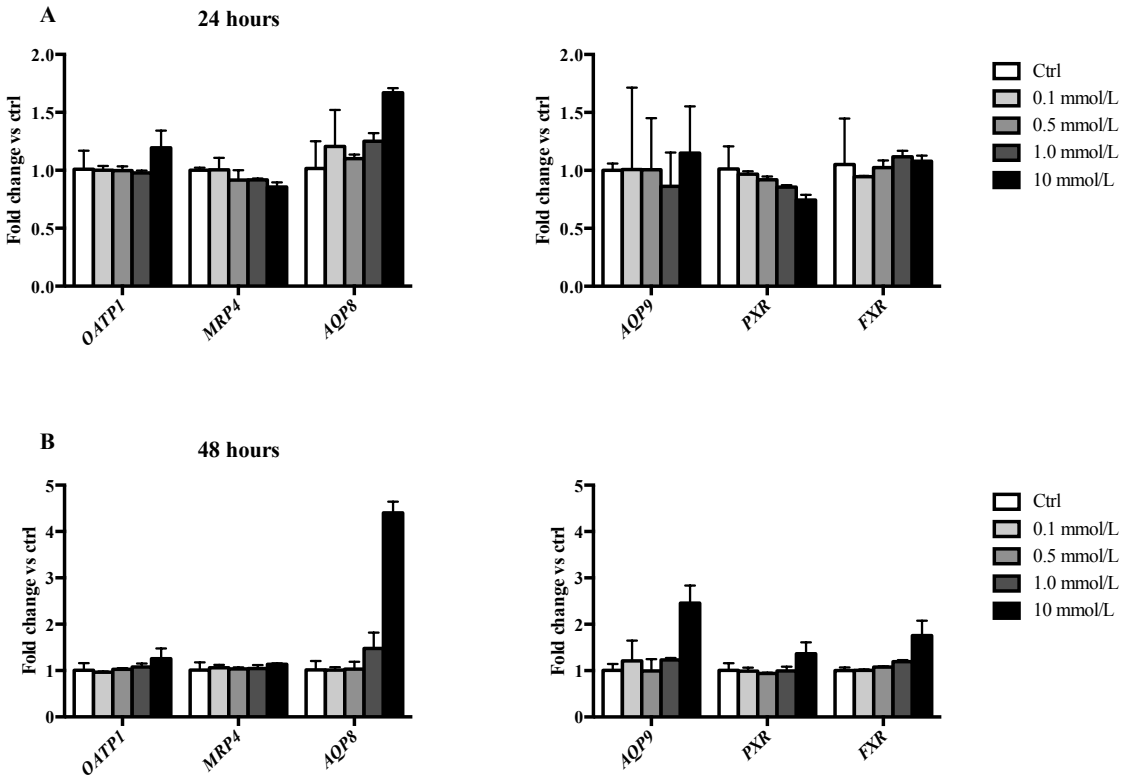

Figure 3.8. **Effect of ammonium chloride on relative mRNA expression level in Hep G2 cells**. The effect of different concentration of ammonium chloride (0.1, 0.5, 1.0, or 10 mmol/L) on relative mRNA expression levels of *OATP1*, *MRP4*, *AQP8*, *AQP9*, *FXR*, and *PXR* in Hep G2 cells (~100.000 cells per well, 12 wells plate, at 37°C with 5% CO_2) were measured after 24 (A), or 48 (B) hours. The data are presented as mean and SD (n=3).

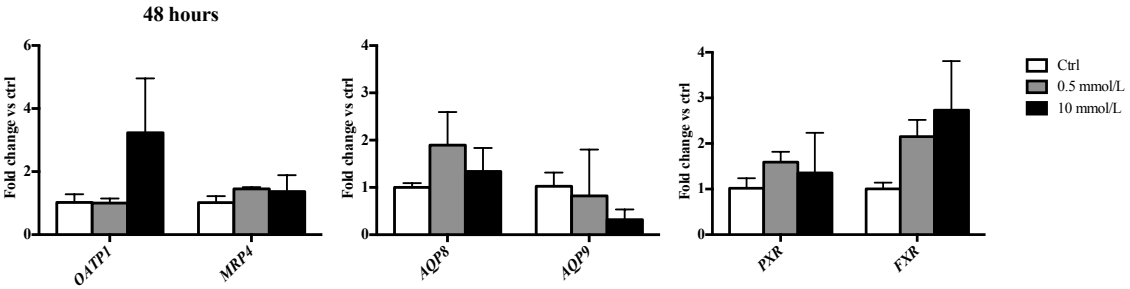

Figure 3.9. **Effect of ammonium chloride on relative mRNA expression level in H1 cells**. The effect of different concentration of ammonium chloride (0.5, or 10 mmol/L) on relative mRNA expression levels of *OATP1, MRP4, AQP8*, *AQP9, PXR*, and *FXR* in H1 cells (~ 440.000 cells per well, 6 wells plate) at 37°C with 5% CO_2) were measured after 48 hours. The data are presented as mean and SD (n=3).

3.4. Single Interfering experiments on Hep G2 cells

3.4.1. Effect of *FXR* knockdown

The expression of *mRNA AQP8* is increased in both Hep G2 and H1 cells after exposure to ammonia. The expression of *FXR* is also increased. To examine whether the expression of *AQP8* is regulated through mechanisms involving the nuclear receptor *FXR*, Hep G2 cells were transfected with siRNA against *FXR*. Three different SiRNA *FXR* have previously been tested by our group and we have selected NR1H4 (FXR) Silencer® Select Pre-designed siRNA cat# 4392420 (Ambion, US) for knock down of *FXR* (data not shown). In the current model transfection with siRNA against *FXR* reduced FXR mRNA level with ~ 80% after 48 hours, and ~ 45% after 72 hours (figure 3.10. and figure 3.11.). Scramble siRNA (Silencer® FAM™ Labeled Negative Control siRNA #1, cat# AM4620) (Ambion, UK) was tested as control, but had unspecific effects on several genes, and thus wells with lipofectamine were used as controls. A new scramble siRNA is to be tested. The expressions of *PXR*, *AQP8*, *OATP1*, or *MRP4* were not changed after transfection with siRNA against *FXR* after 48 or 72 hours. The expression of *AQP9* was not changed after 48 hours, but was increased after 72 hours. However due to low number of replicates at 72 hours (n=2) these result are preliminary and should be interpreted with caution.

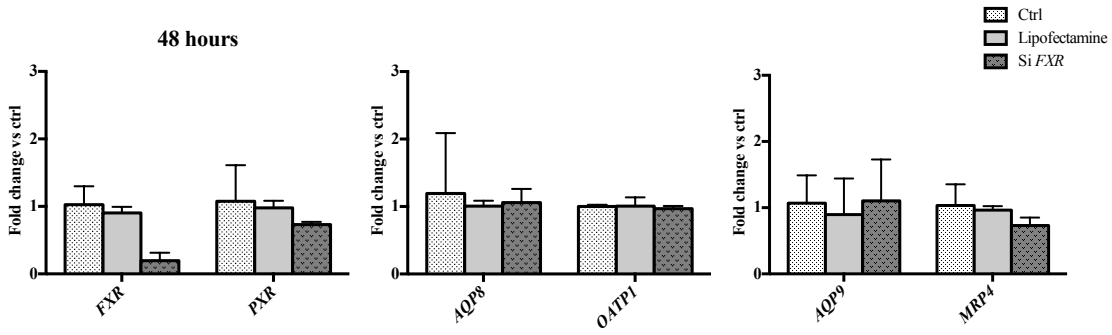

Figure 3.10. **Knockdown of *FXR* in Hep G2 cells**. SiRNA against *FXR*. Relative mRNA expression levels of *FXR*, *PXR*, *AQP8*, *OATP1*, *AQP9*, and *MRP4* in Hep G2 cells (~100.000 cells per well, 12 wells plate) were measured after 48 hours incubation at 37°C with 5% CO2. The data are presented as mean and SD (n=3).

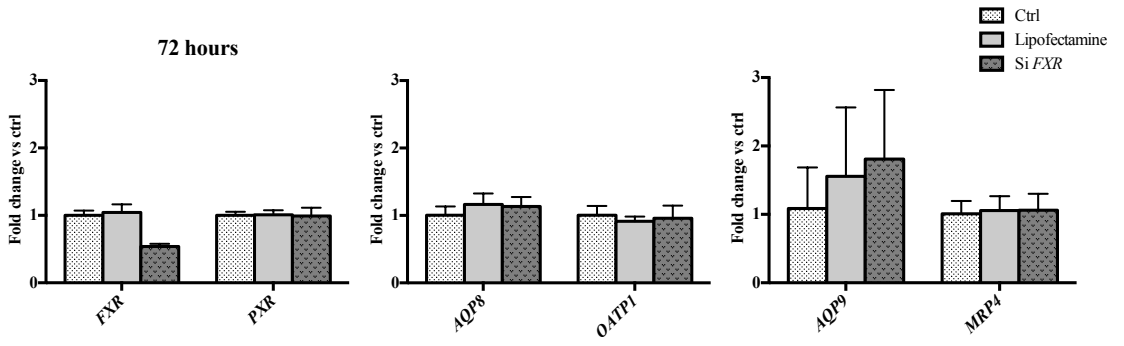

Figure 3.11. **Knockdown of *FXR* in Hep G2 cells**. SiRNA against *FXR*. Relative mRNA expression levels of *FXR*, *PXR*, *AQP8*, *OATP1*, *AQP9*, and *MRP4* in Hep G2 cells (~100.000 cells per well, 12 wells plate) were measured after 72 hours incubation at 37°C with 5% CO2. The data are presented as mean and SD (n=2).

After downregulation of *FXR* by siRNA for 48 hours, Hep G2 cells were exposed to 10 mmol/L ammonium chloride for 24 hours (figure 3.12.). mRNA expression of *PXR*, *AQP8*, *OATP1*, and *MRP4* did not change after ~ 60% knockdown of *FXR*, but *AQP9* was increased compared to both controls and lipofectamine.

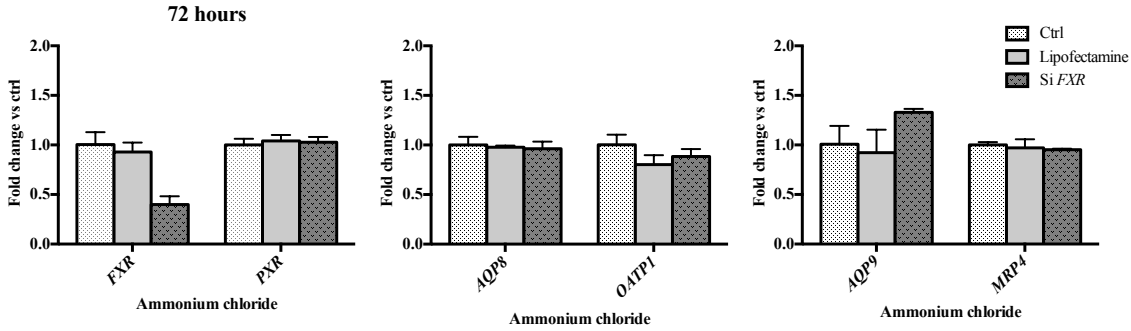

Figure 3.12. **Knockdown of *FXR* in Hep G2 cells exposed to ammonium chloride**. SiRNA against *FXR* in Hep G2 cells (~100.000 cells per well, 12 wells plate) was incubated (37°C with 5% CO_2) for 48 hours before 10 mmol/L ammonium chloride was added and incubated for further 24 hours. Relative mRNA expression levels of *FXR*, *PXR*, *AQP8*, *OATP1*, *AQP9*, and *MRP4* were measured. The data are presented as mean and SD (n=2).

3.4.2. Effect of *AQP8* knockdown

Hep G2 cells transfected with siRNA against *AQP8* (AQP8 Silencer® Select Pre-designed siRNA cat# 4392420 ID: s1485, Ambion, US) caused a ~ 60%

downregulation of *AQP8* mRNA compared to controls (figure 3.13.) after incubation for 72 hours. Expression of *FXR*, *PXR,* and *MRP4* were not affected by *AQP8* knockdown. *OATP1* was downregulated compared to controls and lipofectamine, and *AQP9* was apparently increased after *AQP8* knockdown. However, a low number of replicates (n=2) limits the interpretation of these data. This has to be investigated further.

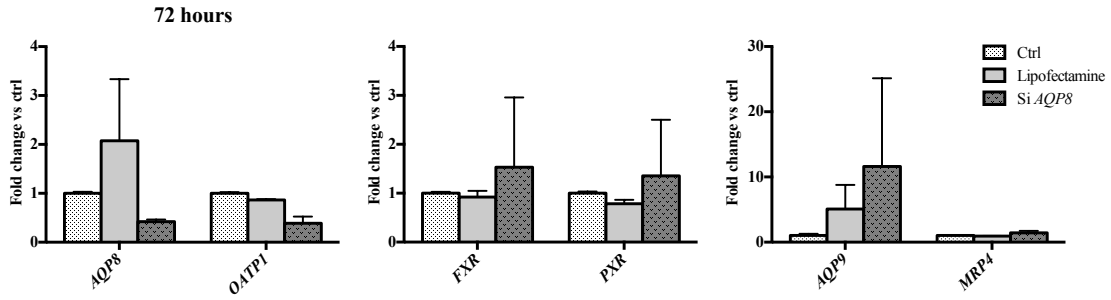

Figure 3.13. **Knockdown of *AQP8* in Hep G2 cells.** SiRNA against *AQP8* in Hep G2 cells (~100.000 cells per well, 12 wells plate) were incubated (37°C with 5% CO_2) for 72 hours. Relative mRNA expression levels of *AQP8, OATP1, FXR*, *PXR*, *AQP9*, and *MRP4* were measured. The data are presented as mean and SD (n=2).

Downregulation of *AQP8* by siRNA for 48 hours followed by exposure to ammonium chloride for 24 hours (figure 3.14.) did not change the expression of *FXR*, *PXR* or *MRP4*, and the effects on *OATP1* and *AQP9* were not different from the effect without ammonium chloride.

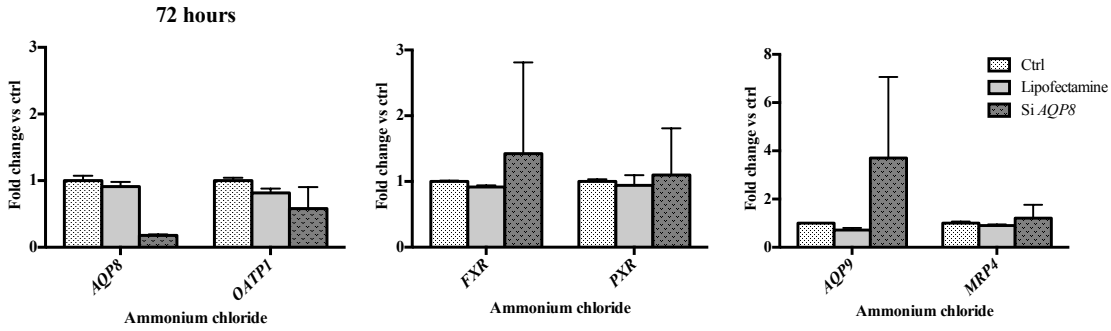

Figure 3.14. **Knockdown of *AQP8* in Hep G2 cells exposed to ammonium chloride**. SiRNA against *AQP8* in Hep G2 cells (~100.000 cells per well, 12 wells plate) were incubated (37°C with 5% CO_2) for 48 hours before 10 mmol/L ammonium chloride was added and incubated for 24 hours. Relative mRNA expression levels of *AQP8, OATP1, FXR*, *PXR*, *AQP9*, and *MRP4* were measured. The data are presented as mean and SD (n=2).

After knockdown of *AQP8* for 48 hours, and exposure for ammonium chloride for 24 hours in Hep G2 cells, mmol/L urea was measured in supernatants and no significant difference between the groups were found (control 5.17 ± 0.18, lipofectamine 5.27 ± 0.14, siRNA against *AQP8* 5.53 ± 0.31), n=3 (p=0.20).

3.5. Effect of ammonia on AQP8 protein expression

3.5.1. AQP8 protein expression in Hep G2 cells

As demonstrated earlier expression of mRNA *AQP8* was increased after exposure for ammonium acetate or ammonium chloride. Protein levels of AQP8 were measured in Hep G2 cells exposed to ammonium chloride for 48, and 72 hours assessed by western blotting. Two bands stained with AQP8 antibody, at the expected 34-36kDa, and an additional band at 70kDa in some lanes at both 48 (figure 3.15.), and 72 (figure 3.17.) hours. The latter was interpreted as a dimer of the monomer, and both bands were included in the calculations (figure 3.16. for 48 hours, and figure 3.18. for 72 hours). The values were normalized to β-Actin. Ammonium chloride did not significantly change the protein level of AQP8 in Hep G2 cells after 48 (p=0.414, n=3), and 72 hours (p=0.053, n=4).

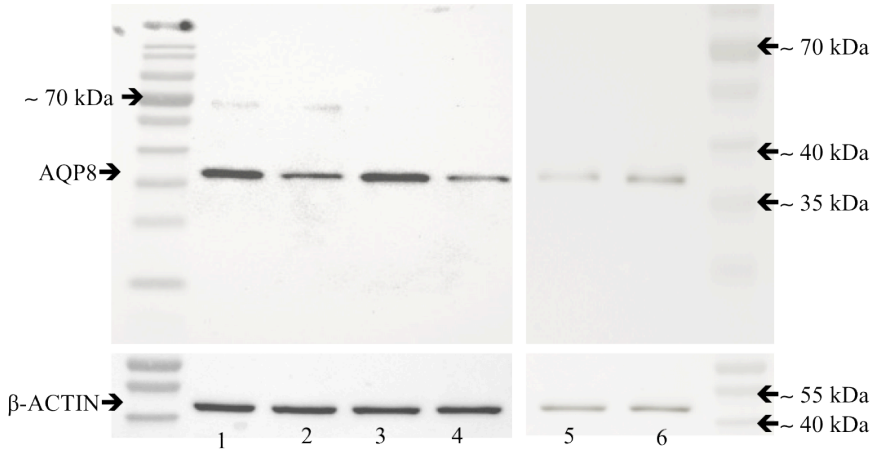

Figure 3.15. **AQP8 expression in Hep G2 cells**. Control samples in lane 1, 3, and 5, and samples exposed to 10 mmol/L ammonium chloride are shown in lane 2, 4, and 6 after incubation (37°C with 5% CO_2) for 48 hours. AQP8 (molecular weight 34 kDa) is shown ~ 36 kDa. β-ACTIN (molecular weight 43 kDa) is shown at ~ 43 kDa.

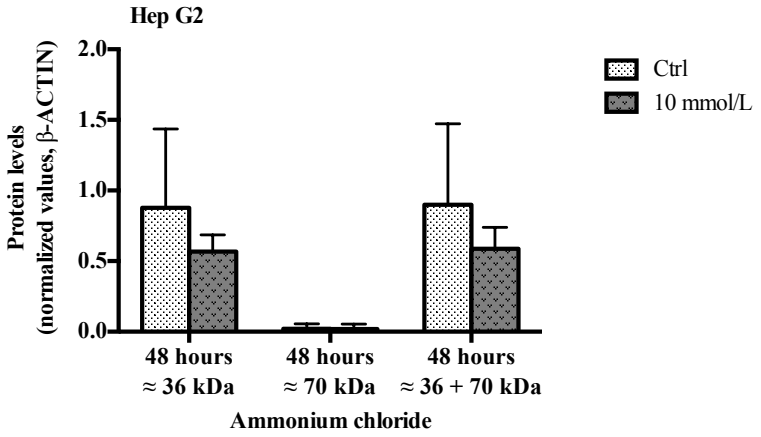

Figure 3.16. **Relative quantification of AQP8 in Hep G2 cells**. Western blotting was used to quantify relative expression of AQP8 in Hep G2 cells after 48 hours when exposed to 10 mmol/L ammonium chloride. β-ACTIN was used to normalize data, presented as mean and SD (n=3).

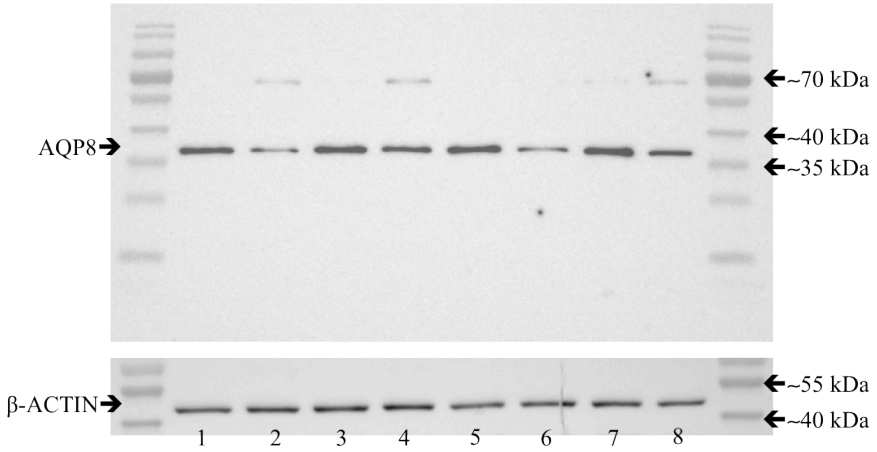

Figure 3.17. **AQP8 expression in Hep G2 cells.** Control samples are shown in lane 1, 3, 5, and 7, and samples exposed to 10 mmol/L ammonium chloride in lane 2, 4, 6, and 8 after incubation (37°C with 5% CO_2) for 72 hours. AQP8 (molecular weight 34 kDa) is shown ~ 36 kDa. β-ACTIN (molecular weight 43 kDa) is shown at ~ 45 kDa.

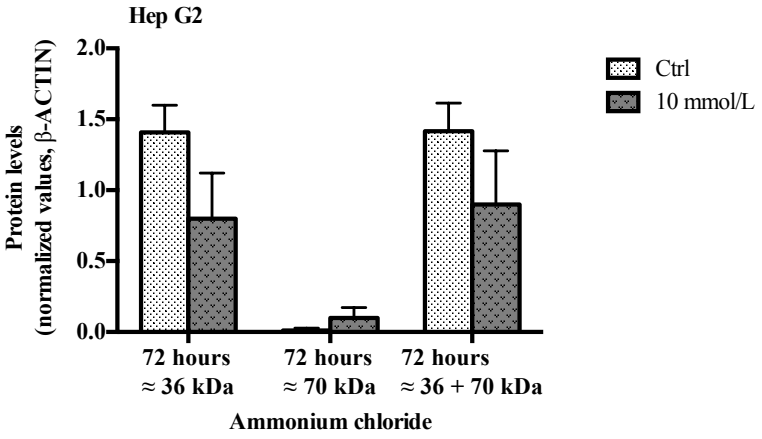

Figure 3.18. **Relative quantification of AQP8 in Hep G2 cells**. Western blotting was used to quantify relative expression of AQP8 in Hep G2 cells after 72 hours. β-ACTIN was used to normalize data, presented as mean and SD (n=4).

3.5.2. AQP8 protein expression in H1 cells

In H1 cells exposed to 10 mmol/L ammonium chloride, as for Hep G2, two band appeared: at expected on 34-36kDa, and at 70kDa (figure 3.19.). Both bands were included in the calculations (figure 3.20.). Ammonium chloride AQP8 appeared to be increased in H1 cells after 72 hours, not significantly (p=0.342, n=3).

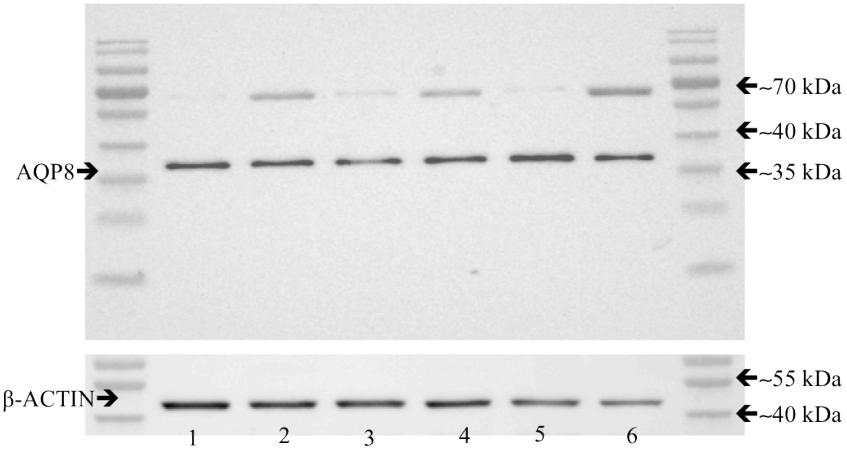

Figure 3.19. **AQP8 expression in H1 cells**. Control samples are shown in lane 1, 3, and 5, and samples exposed to 10 mmol/L ammonium chloride for 72 hours are shown in lane 2, 4, and 6. A band assumed to represent AQP8 (molecular weight 34 kDa) appeared at ~ 36 kDa.

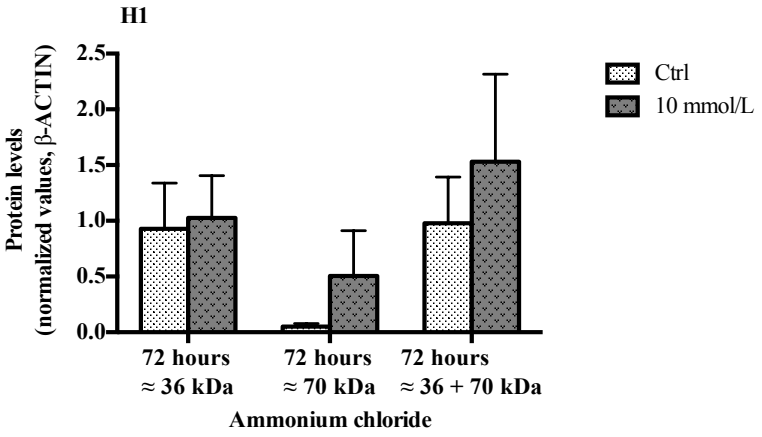

Figure 3.20. **Relative quantification of AQP8 in H1 cells**. Western blotting was used to quantify relative expression of AQP8 in H1 cells after 72 hours in cells exposed to 10 mmol/L ammonium chloride and controls. β-ACTIN was used to normalize data, presented as mean and SD (n=3).

Chapter 4

Discussion

4.1. Morphology and cell function

4.1.1. Ammonia detoxification

Cell cultures are frequently used for *in vitro* analyses to study the effect of drugs and toxicity in different tissues and organs, and the consistency and ability to reproduce is an important advantage. To find a hepatic cell line that could be obtained in large quantities and with the ability to remove ammonia is of great clinical importance in the development of bioartificial liver devices (Mavri-Damelin et al. 2008). Several systems based on dialyses and filtration are now used as short-term "bridges to transplantation" to remove ammonia and other toxins in patients with acute and chronic liver failure, but there is an ongoing work to make devices based on hepatocytes (Phua & Lee 2008). Selecting a cell line, which has the required features such as biotransformatory functions and the ability to detoxify ammonia, has been challenging.

Hep G2, human hepatocellular carcinoma, cells are often used as a model system in research of liver function. This cell line is virus free, easy to obtain in large quantities, has a high extent of morphologic and functional differentiation (Tyakht et al. 2014), and is used to study metabolism, gene expression and toxicity. The metabolic activity of Hep G2 is generally lower than in human primary hepatocytes (Balls et al. 2012). Human primary hepatocytes are more difficult to obtain. Other disadvantages are changes in morphology, structure, and liver-specific functions in a few days/passage

(Shulman & Nahmias 2013;Soldatow et al. 2013). While Hep G2 cells are available in large quantities, they have a limited capacity to remove ammonia.
Low expression of the urea cycle enzymes ornithine transcarbamylase (OTC) and arginase I has been the explanation for low urea production in Hep G2 cells (Mavri-Damelin et al. 2007). Transfection with these two enzymes restored urea cycle activity in Hep G2, indicating that the other enzymes in the urea cycle were fully functional (Mavri-Damelin et al. 2007;Tang et al. 2012). Mavri-Damelin et al. speculated whether hepatocyte nuclear factor 4, highly expressed in Hep G2 cells, inhibited the expression of arginase I, and that the low OTC level is due to a promotor hypermethylation, based on reversed expression of OTC after treatment with a demethylating agent (Mavri-Damelin et al. 2006). A similar mechanism was demonstrated in human hepatocellular carcinoma (HCC) cells (LH88, and Huh7), which do not express carbamoyl phosphate synthetase 1 (CPS1). The expression of CPS1 was restored by treatment of a demethylating agent (Liu et al. 2011). C3A, a subclone of Hep G2, have the ability to produce urea, but the formation of urea is due to arginase II activity rather than urea cycle activity. Arginase II, an enzyme that produces urea independently of the urea cycle is increased in C3A, and is also present in Hep G2 (Mavri-Damelin et al. 2008). Primary porcine hepatocytes demonstrate higher cytochrome P450 activity, and ammonia removal than C3A. The disadvantages of concern in addition to metabolic functions in tumorigenic cells are the decreased ability in immunocompromised patients to remove malignant cells from circulation. In xenogenic hepatocytes the concerns are immunogenicity, zoonoses and biocompability (Tsiaoussis et al. 2001).

Tang et al. illustrated that LD50 (lethal dose) for Hep G2 cells exposed to ammonium chloride was reached at 60 mmol/L (100.000 cells per well), and that stable overexpression with arginase I and OTC increased the capacity for ammonia tolerance to three times to that of native Hep G2 (Tang et al. 2012). We did find a significant urea production (4.4 mmol/L) in Hep G2 cells after exposure of 10 mmol/L ammonium chloride for 48 hours. This is somewhat higher than the concentration reported by Tang et al (1.8 mmol/L). Tang et al. used a shorter incubation time (12 hours) compared to our experiments (48 hours), and this could partly explain the difference. Furthermore, they also used higher concentration of ammonium chloride (60-480 mmol/L) compared to our experiments (0.5 or 10 mmol/L). Tang et al. found that the urea formation decreased with increasing doses of ammonium chloride. Taken together, our

experiments and the experiments published by Tang et al. suggest a bell shaped relation between concentration of ammonia and production of urea in Hep G2. While the urea cycle is the major system for production of urea in the liver, as mention above, urea can also be produced from arginase II (Mavri-Damelin et al. 2007). Whether urea was produced from urea cycle or from arginase II in our experiments has not been determined yet. Hoekstra et al. found a marked increase in urea formation in HepRg cells after incubation with plasma from acute-liver-failure rats, change in total ammonia elimination, and decreased urea cycle activity. The increase in urea was due to increased urea production from arginine by upregulated arginase II activity (Hoekstra et al. 2012). This may be the explanation for the increased production of urea in the Hep G2 cell as well. We also tested the ability to produce urea in another cell line, stem cells derived to hepatocyte-like cells, H1. H1cells produced urea both at 0.5 and 10 mmol/L ammonium chloride. A similar increase in urea formation with increasing dose of ammonium chloride was found as in Hep G2.

4.1.2. Effect of ammonia on viability

Neurotoxic effects of ammonia have been emphasized in patients with liver failure rather than the potential hepatotoxic effects. However, patients with repeated exposures to high ammonia levels exhibit liver damage (Jia et al. 2014;Yaplito-Lee et al. 2013). We demonstrate that ammonia reduces metabolic activity in Hep G2 cells measured by MTT. There was no difference between the toxic effect of ammonium acetate and ammonium chloride, indicating that the cell damage is caused by ammonium and not by acetate or chloride. This is in line with the experiments published by Tang et al. who found that LD50 for Hep G2 cells was 60 mmol/L.

As mentioned, Hep G2 has a low basal production of urea due to low levels of OTC and arginase I. One could argue that Hep G2 has limitations as a model system for studying ammonia toxicity as the absent or low basal urea cycle activity would render the Hep G2 cells more susceptible to ammonia toxicity than cell lines with a functioning urea cycle. At a high concentration of ammonium chloride (60 mmol/L) cell viability is higher in Hep G2 cell overexpressed with OTC and arginase I than in Hep G2 (Tang et al. 2012). The experiments performed by Tang et al. demonstrated that Hep G2 overexpressing OTC and arginase I, that had a functioning urea cycle, also was

damaged by ammonia, but to a lesser extent. Whether these differences also persist at lower concentrations of ammonia is undetermined. Thus there is certainly a quantitative difference in the response to ammonia toxicity between hepatocytes with and without/with low urea cycle activity. However, one should keep in mind that in the clinical situation some of the patients have impaired (as in liver failure) or no urea cycle activity (urea cycle defects) (Bernal et al. 2010;Hoekstra et al. 2012;Rudman et al. 1973). In these situations the liver with no, or reduced, urea cycle activity is exposed to high concentrations of ammonia. Thus we consider the Hep G2 to be a relevant model for assessment of ammonia toxicity. Ammonia toxicity was also studied in H1 cells and increased amount of AST indicates cell damage due to treatment of ammonia compared to controls. ALT was also measured in both cell lines, but the method used was not sensitive enough to detect levels produced from the chosen amount of cells (100.000 cells per well).

While ammonia causes neuronal toxicity by predominately affecting astrocytes (Felipo & Butterworth 2002), less is known about the mechanisms for ammonia associated liver toxicity. Wang et al. found that ammonia increased mitochondrial permeability, reduced TCA cycle intermediates and ATP release, and increased apoptosis (Wang et al. 2014). Jia et al. also found increased hepatic apoptosis associated with enhanced expression of cyclin D1 and A (Jia et al. 2014).

Hyperammonemia is defined as plasma levels > 50 mmol/L (Haberle 2013). Clinically, some patients experience plasma/serum ammonia concentrations up to 2000 μmol/L (Yaplito-Lee et al. 2013). In this study the concentrations range from 0.1 to 10 mmol/L of ammonia. Our result from cell viability measurements on Hep G2 arrayed ammonium chloride and ammonium acetate to be clearly toxic at 10 mmol/L. The H1 cells also demonstrated increased AST levels at 0.5 mmol/L. Thus the concentrations we have tested are at the high levels, and above, of what is measured in the serum of patients. On the other hand we also demonstrated that increased time of exposure resulted in more pronounced damage. This is in line with the findings of Wang et al. Jia et al. found that AST and ALT levels increased with increasing time in a model with intragastric ammonium chloride in rats. In this model the ammonia levels was about 120 μmol/L (Jia et al. 2014). Thus lower, and clinically relevant, concentrations of ammonia may cause damage to the hepatocyte when the time of exposure is extended.

4.2. Effect of ammonia on gene expression in the liver

As stated, ammonia may have deleterious effects on the liver, but it is also possible that ammonia causes changes that are beneficial in a situation with liver failure and may have damage-modifying effects. To explore this we examined the effects of ammonium chloride on expression of selected genes. Previously, Jia et al. have found that hyperammonemia caused differentially expression of 198 genes more than 2 fold change, with 63 up-regulated and 135 down-regulated genes. This included genes involved in regulation of biological and cellular processes, cell communication, and immune response (Jia et al. 2014). Other studies are more targeted. Wang et al. found that 10 mmol/L ammonia caused a reduction of mRNA level of multidrug resistance protein 2 (*MRP2*) (Wang et al. 2014). We studied the effects of ammonia on two nuclear receptors (*PXR* and *FXR*), two aquaporins (*AQP8* and *AQP9*) and two hepatobiliary transport systems (*OATP1* and *MRP4*) in Hep G2 and H1 cells.

Pregnane X receptor (PXR) and farnesoid X receptor (FXR) are both ligand-activated nuclear receptors, highly expressed in the liver and intestines, and several genes are regulated by these receptors (Zollner & Trauner 2009). PXR is central for regulation of xenobiotic metabolism, including oxidation, conjugation and transport (Kliewer et al. 2002), and FXR is essential for regulation of endobiotics, bile acid uptake, metabolism, and excretion (Fiorucci et al. 2012). Earlier studies by Renga et al. have shown that activation of FXR regulates the metabolism of glutamine and glutamate in primary hepatocytes obtained from mice, and FXR ligands may be useful in treatment of hyperammonemia due to increased induction of NAGS and glutamate – and glutamine transporters (Renga et al. 2011). As far as we know ammonias direct effect on these receptors in Hep G2 cells is unknown. Our results showed no markedly change in mRNA expression of *PXR* in both Hep G2 and H1 after treatment of both 10 mmol/L ammonium chloride and ammonium acetate. mRNA expression of *FXR* was slightly upregulated after 48 hours in both cell lines, indicating that ammonia may affect *FXR*. Although the expression of *FXR* was increased after ammonia it does not necessarily mean that *FXR* is activated. To investigate this further a FXR reporter assay could be used to examine the agonism or antagonism of FXR.

Aquaporins (AQPs), ubiquitous small membrane channels, contribute to maintain homeostasis by facilitating water and uncharged substances across the membranes. AQP0-12 have been identified in mammals and are classified in three groups according to permeability: 1) permeable to water, 2) permeable to water, ammonia, glycerol, and urea, and 3) permeable to water and ammonia. AQPs in addition to rhesus-type (Rh) proteins contribute to transport of ammonia (Geyer et al. 2013;Weiner & Verlander 2010). In mouse liver AQP8 is located in the canalicular plasma membrane, in intracellular vesicles, and in mitochondria (Calamita et al. 2005;Ferri et al. 2003), whereas AQP9 (group 2) is located on the sinusoidal side in the plasma membrane in hepatocytes. AQP9 takes part in NH_3 uptake, and efflux of newly synthesised urea (Geyer et al. 2013).

Larocca et al. confirmed that AQP8 was present in Hep G2 cells, and Marchissio et al. demonstrated AQP8 in the inner mitochondrial membrane in Hep G2 cells, mtAQP8 (Larocca et al. 2009;Marchissio et al. 2012). In our study both ammonium chloride and ammonium acetate caused a significant increase in expression of *AQP8* at mRNA level both after 48 and 72 hours. There was also a tendency to increased *AQP8* expression in H1 cells after ammonium chloride exposure.

As mentioned above *FXR* expression was also affected by ammonia. To examine whether *AQP8* was regulated via this nuclear receptor we performed knockdown *FXR*. In Hep G2 cells the effect of knockdown with 20 nmol/L siRNA was ~ 80% and ~ 45% after 48 and 72 hours, respectively. *AQP8* was unaffected after both 48 and 72 hours, indicating that *AQP8* was not regulated via *FXR* signalling pathway. Optimal knockdown depends on siRNA concentration, cell type, and time of transfection. Due to an increase in *FXR* expression after knockdown after 72 hours compared to 48, re-transfection after 48 hours should be performed. Considering that we have a low number of replicates at 72 hours (n=2) these results should be interpreted with caution. However, Van Erpecum et al. found no difference in *AQP8* expression in *FXR* deficient mice and wild type mice after one week on lithogenic diet, containing FXR ligand cholic acid (van Erpecum et al. 2006), supporting our results.

As mRNA of *AQP8* was markedly enhanced by ammonium chloride and ammonium acetate we also assessed AQP8 protein levels after exposure to ammonium chloride. Two bands stained, using a specific antibody, at expected 34-36 kDa, and in lane 70 kDa. The bands in lane 70 kDa are interpreted as dimerization of AQP8. The results are

calculated separately, and added together (chapter 3.5.). Both Hep G2 and H1 showed the same tendency in terms of dimerization. Whether dimerization was due to ammonia itself or due to the method used for isolation of proteins is not yet determined. Other studies have also shown that AQPs tend to form dimers (Blanc et al. 2009;Laforenza et al. 2005;Laforenza et al. 2009). In Hep G2 the protein level of AQP8 was decreased after both 48 and 72 hours. In contrast an increase protein level of AQP8 was found in H1 cells. The increased mRNA level and decreased protein levels have also been found in other studies. Wang et al. found increased mRNA level of *AQP8,* and decreased protein levels of AQP8 in septic-induced rats (Wang et al. 2013). Carreras et al. studied AQP8 expression in rats with extrahepatic cholestasis. They found unaffected mRNA and protein expression after one day in rats with bile duct ligation. However, after 3 and 7 days the protein level was decreased in contrast to increase mRNA (Carreras et al. 2003). Further they found downregulation of AQP8 protein in estrogen- induced cholestasis, whereas *AQP8* mRNA level was increased (Carreras et al. 2007). *In vivo* studies in rats, and *in vitro* studies of primary cultured hepatocytes increased AQP8 protein levels after stimulation of glucagon. mRNA levels were unchanged, and they suggested that glucagon induces the gene expression of rat hepatocyte AQP8 protein by reducing its degradation (Soria et al. 2009). Increased *AQP8* mRNA level, and downregulated protein expression indicates involvement of posttranscriptional mechanisms, or increased degradation of protein. As far as we know the half-life of AQP8 protein is unknown, and a possibility is that ammonia leads to an increased degradation of AQP8 protein, and also a reduction in half-life.

After knockdown of mitochondrial *AQP8* (mt*AQP8*) Soria et al. found reduced basal ureagenesis in primary rat hepatocytes, and increased ammonia levels after 48 hours. Knockdown of mt*AQP8* also decreased urea production stimulated by glucagon, and ammonium chloride (1.0 mmol/L) (Soria et al. 2013). Our results show that *AQP8* mRNA expression was increased after exposure to 10 mmol/L ammonium acetate and ammonium chloride in Hep G2 cells after 24, and 48 hours, and H1 cells after 48 hours. Increased urea production was detected in both cell lines. However urea production in supernatants from Hep G2 cells after knockdown of *AQP8* was unaffected. In our experiments 72 hours of incubation with siRNA against *AQP8* resulted in a 60% decrease in mRNA levels of *AQP8*. Whether this also resulted in a decrease in AQP8 protein levels was not determined and thus the lack of effect of siRNA against *AQP8* on

urea formation should be interpreted with caution. Furthermore the concomitant exposure ammonium chloride may have changed the protein levels of AQP8 in these experiments. Thus these data have to be followed by additional experiments to be conclusive.

AQP9 is permeable to water, ammonia, glycerol, and is an efflux channel of urea (Geyer et al. 2013). We found increased mRNA level of *AQP9* in Hep G2, and decreased mRNA levels in H1 cells after ammonia treatment for 48 hours. The increased levels may correspond to the findings of Jelen et al. They found decreased levels of urea and ammonia in plasma and liver in *AQP9* deficient murine after high protein diet, and that AQP9 contributes to removal of urea from the liver (Jelen et al. 2012). To investigate whether AQP9 is translated to proteins, protein quantification assessed by e.g. western blotting could be performed.

Organic anion transporting polypeptides (OATPs) mediates cellular uptake of various substrates, such as bile acids, steroid conjugates, and xenobiotics. OATPs are located in different tissues, including liver on the basolateral membrane in hepatocytes (Roth et al. 2012). mRNA level of *OATP1* (SLCO4A1) was increased in Hep G2 cells after 24 hours, and in H1 after 48 hours when exposed to 10 mmol/L ammonia. As far as we know there is little research on ammonias effect on OATP1. Some OATPs is regulated via FXR, e.g. OATP8, exclusively expressed in the basolateral membrane of hepatocytes (Ohtsuka et al. 2006). There was no up or down regulation in *OTAP1* after knockdown of *FXR*, indicating no regulation via *FXR*. *OATP1* and *AQP8* are increased after exposure for 10 mmol/L ammonia, and both are decreased after knockdown of *AQP8* in Hep G2 cells, illustrating a similar pattern in presence of ammonia. *AQP8* and *OATP1* in humans are located on chromosome 16 and 20, respectively (NCBI 2015a;NCBI 2015b). To investigate whether the downregulation of *OATP1* is due to random binding, several siRNA against *AQP8* could be used. Due to a low number of replicates (n=2) these result are preliminary and should be interpreted with caution.

Multidrug resistance protein 4 (MRP4) is an efflux transporter located on the basolateral membrane in hepatocytes (Borst et al. 2007). The main function is to eliminate bile acids. *MRP4* was unaffected after exposure to 10 mmol/L ammonia in both Hep G2 and H1cells, and after knockdown of *FXR*. The latter finding is in keeping with data from

Wagner et al. indicating that MRP4 is regulated independently from FXR (Wagner et al. 2003).

In summary the data presented show that ammonia affects hepatocytes, both Hep G2 and H1 cells. Both cell lines have reduced metabolic activity, and increased urea production after exposure to ammonia. Ammonia also regulates gene expression by increasing mRNA level of *AQP8* and *OATP1*. However, in Hep G2 AQP8 protein expression was downregulated. Taken together, Hep G2 and H1 cells had relatively similar expression patterns on the selected genes.

4.4. Future aspects

In this study we found that ammonia affects cell damage and metabolic activity in H1 hepatocytes and Hep G2 cells. Ammonia also causes changes in expression of some genes in hepatocytes. We want to explore this further. First we have to repeat several of the experiments, and in the siRNA experiments a new scramble control has to be tested. A particular interesting aspect was the pronounced increase in *AQP8* mRNA contrasting the lack of increase in AQP8 protein levels. We want to explore this further by studying whether this is due to posttranscriptional changes. Furthermore we want to perform subcellular fractionation to distinguish between mitochondrial AQP8 and cytosolic AQP8 in Hep G2 cells and how this relation is affected by ammonia.
We also want to study AQP9 and OATP1 at a protein level and further explore the mechanisms of cell damage exerted by ammonia in hepatocytes.

Literature

Abacan, M. & Boneh, A. (2013). Use of carglumic acid in the treatment of hyperammonaemia during metabolic decompensation of patients with propionic acidaemia. *Mol Genet Metab*, 109 (4): 397-401.

Adeva, M. M., Souto, G., Blanco, N. & Donapetry, C. (2012). Ammonium metabolism in humans. *Metabolism*, 61 (11): 1495-511.

Al Sibae, M. R. & McGuire, B. M. (2009). Current trends in the treatment of hepatic encephalopathy. *Ther Clin Risk Manag*, 5 (3): 617-26.

Badizadegan, K. & Perez-Atayde, A. R. (1997). Focal glycogenosis of the liver in disorders of ureagenesis: its occurrence and diagnostic significance. *Hepatology*, 26 (2): 365-73.

Balls, M., Bhogal, N., Combes, R. D. & SpringerLink (Online service). (2012). *New Technologies for Toxicity Testing*. Advances in Experimental Medicine and Biology. New York, NY: Springer US.

Bernal, W., Auzinger, G., Dhawan, A. & Wendon, J. (2010). Acute liver failure. *Lancet*, 376 (9736): 190-201.

Blanc, L., Liu, J., Vidal, M., Chasis, J. A., An, X. & Mohandas, N. (2009). The water channel aquaporin-1 partitions into exosomes during reticulocyte maturation: implication for the regulation of cell volume. *Blood*, 114 (18): 3928-34.

Borst, P., de Wolf, C. & van de Wetering, K. (2007). Multidrug resistance-associated proteins 3, 4, and 5. *Pflugers Arch*, 453 (5): 661-73.

Calamita, G., Ferri, D., Gena, P., Liquori, G. E., Cavalier, A., Thomas, D. & Svelto, M. (2005). The inner mitochondrial membrane has aquaporin-8 water channels and is highly permeable to water. *J Biol Chem*, 280 (17): 17149-53.

Capistrano-Estrada, S., Marsden, D. L., Nyhan, W. L., Newbury, R. O., Krous, H. F. & Tuchman, M. (1994). Histopathological findings in a male with late-onset ornithine transcarbamylase deficiency. *Pediatr Pathol*, 14 (2): 235-43.

Carreras, F. I., Gradilone, S. A., Mazzone, A., Garcia, F., Huang, B. Q., Ochoa, J. E., Tietz, P. S., Larusso, N. F., Calamita, G. & Marinelli, R. A. (2003). Rat hepatocyte aquaporin-8 water channels are down-regulated in extrahepatic cholestasis. *Hepatology*, 37 (5): 1026-33.

Carreras, F. I., Lehmann, G. L., Ferri, D., Tioni, M. F., Calamita, G. & Marinelli, R. A. (2007). Defective hepatocyte aquaporin-8 expression and reduced canalicular membrane water permeability in estrogen-induced cholestasis. *Am J Physiol Gastrointest Liver Physiol*, 292 (3): 905-12.

Cichoz-Lach, H. & Michalak, A. (2013). Current pathogenetic aspects of hepatic encephalopathy and noncirrhotic hyperammonemic encephalopathy. *World J Gastroenterol*, 19 (1): 26-34.

Ciecko-Michalska, I., Szczepanek, M., Slowik, A. & Mach, T. (2012). Pathogenesis of hepatic encephalopathy. *Gastroenterol Res Pract*, 2012: 642108.

Felipo, V. & Butterworth, R. F. (2002). Neurobiology of ammonia. *Prog Neurobiol*, 67 (4): 259-79.

Ferenci, P., Lockwood, A., Mullen, K., Tarter, R., Weissenborn, K. & Blei, A. T. (2002). Hepatic encephalopathy--definition, nomenclature, diagnosis, and quantification: final report of the working party at the 11th World Congresses of Gastroenterology, Vienna, 1998. *Hepatology*, 35 (3): 716-21.

Ferri, D., Mazzone, A., Liquori, G. E., Cassano, G., Svelto, M. & Calamita, G. (2003). Ontogeny, distribution, and possible functional implications of an unusual aquaporin, AQP8, in mouse liver. *Hepatology*, 38 (4): 947-57.

Fiorucci, S., Mencarelli, A., Distrutti, E. & Zampella, A. (2012). Farnesoid X receptor: from medicinal chemistry to clinical applications. *Future Med Chem*, 4 (7): 877-91.

Geyer, R. R., Musa-Aziz, R., Qin, X. & Boron, W. F. (2013). Relative CO(2)/NH(3) selectivities of mammalian aquaporins 0-9. *Am J Physiol Cell Physiol*, 304 (10): 985-94.

Goldbecker, A., Buchert, R., Berding, G., Bokemeyer, M., Lichtinghagen, R., Wilke, F., Ahl, B. & Weissenborn, K. (2010). Blood-brain barrier permeability for ammonia in patients with different grades of liver fibrosis is not different from healthy controls. *J Cereb Blood Flow Metab*, 30 (7): 1384-93.

Goodsell, D. S. (2005). The molecular perspective: L-asparaginase. *Oncologist*, 10 (3): 238-9.

Haberle, J. (2013). Clinical and biochemical aspects of primary and secondary hyperammonemic disorders. *Arch Biochem Biophys*, 536 (2): 101-8.

Hoekstra, R., Nibourg, G. A., van der Hoeven, T. V., Ackermans, M. T., Hakvoort, T. B., van Gulik, T. M., Oude Elferink, R. P. & Chamuleau, R. A. (2012). The effect of rat acute-liver-failure plasma on HepaRG cells. *Int J Artif Organs*, 35 (11): 1006-14.

Holm, L. M., Jahn, T. P., Moller, A. L., Schjoerring, J. K., Ferri, D., Klaerke, D. A. & Zeuthen, T. (2005). NH3 and NH4+ permeability in aquaporin-expressing Xenopus oocytes. *Pflugers Arch*, 450 (6): 415-28.

Jelen, S., Gena, P., Lebeck, J., Rojek, A., Praetorius, J., Frokiaer, J., Fenton, R. A., Nielsen, S., Calamita, G. & Rutzler, M. (2012). Aquaporin-9 and urea transporter-A gene deletions affect urea transmembrane passage in murine hepatocytes. *Am J Physiol Gastrointest Liver Physiol*, 303 (11): 1279-87.

Jia, B., Yu, Z. J., Duan, Z. F., Lu, X. Q., Li, J. J., Liu, X. R., Sun, R., Gao, X. J., Wang, Y. F., Yan, J. Y., et al. (2014). Hyperammonaemia induces hepatic injury with alteration of gene expression profiles. *Liver Int*, 34 (5): 748-58.

Kim, H. Y. (2009). Renal handling of ammonium and Acid base regulation. *Electrolyte Blood Press*, 7 (1): 9-13.

Kliewer, S. A., Goodwin, B. & Willson, T. M. (2002). The nuclear pregnane X receptor: a key regulator of xenobiotic metabolism. *Endocr Rev*, 23 (5): 687-702.

LaBrecque, D. R., Latham, P. S., Riely, C. A., Hsia, Y. E. & Klatskin, G. (1979). Heritable urea cycle enzyme deficiency-liver disease in 16 patients. *J Pediatr*, 94 (4): 580-7.

Laforenza, U., Cova, E., Gastaldi, G., Tritto, S., Grazioli, M., LaRusso, N. F., Splinter, P. L., D'Adamo, P., Tosco, M. & Ventura, U. (2005). Aquaporin-8 is involved in water transport in isolated superficial colonocytes from rat proximal colon. *J Nutr*, 135 (10): 2329-36.

Laforenza, U., Gastaldi, G., Polimeni, M., Tritto, S., Tosco, M., Ventura, U., Scaffino, M. F. & Yasui, M. (2009). Aquaporin-6 is expressed along the rat gastrointestinal tract and upregulated by feeding in the small intestine. *BMC Physiol*, 9: 18.

Larocca, M. C., Soria, L. R., Espelt, M. V., Lehmann, G. L. & Marinelli, R. A. (2009). Knockdown of hepatocyte aquaporin-8 by RNA interference induces defective bile canalicular water transport. *Am J Physiol Gastrointest Liver Physiol*, 296 (1): 93-100.

Lazier, J., Lupichuk, S. M., Sosova, I. & Khan, A. A. (2014). Hyperammonemic encephalopathy in an adenocarcinoma patient managed with carglumic acid. *Curr Oncol*, 21 (5): 736-9.
Litman, T., Sogaard, R. & Zeuthen, T. (2009). Ammonia and urea permeability of mammalian aquaporins. *Handb Exp Pharmacol* (190): 327-58.
Liu, H., Dong, H., Robertson, K. & Liu, C. (2011). DNA methylation suppresses expression of the urea cycle enzyme carbamoyl phosphate synthetase 1 (CPS1) in human hepatocellular carcinoma. *Am J Pathol*, 178 (2): 652-61.
Maestri, N. E., Brusilow, S. W., Clissold, D. B. & Bassett, S. S. (1996). Long-term treatment of girls with ornithine transcarbamylase deficiency. *N Engl J Med*, 335 (12): 855-9.
Marchissio, M. J., Frances, D. E., Carnovale, C. E. & Marinelli, R. A. (2012). Mitochondrial aquaporin-8 knockdown in human hepatoma HepG2 cells causes ROS-induced mitochondrial depolarization and loss of viability. *Toxicol Appl Pharmacol*, 264 (2): 246-54.
Matoori, S. & Leroux, J. C. (2015). Recent advances in the treatment of hyperammonemia. *Adv Drug Deliv Rev*.
Mavri-Damelin, D., Eaton, S., Coward, S., Damelin, L., Rees, M., Selden, C. & Hodgson, H. J. F. (2006). Restoring urea cycle function in HepG2 cells by multiple gene transfer; A cell source for a bio-artificial liver device. *Journal of Hepatology*, 44: 144.
Mavri-Damelin, D., Eaton, S., Damelin, L. H., Rees, M., Hodgson, H. J. & Selden, C. (2007). Ornithine transcarbamylase and arginase I deficiency are responsible for diminished urea cycle function in the human hepatoblastoma cell line HepG2. *Int J Biochem Cell Biol*, 39 (3): 555-64.
Mavri-Damelin, D., Damelin, L. H., Eaton, S., Rees, M., Selden, C. & Hodgson, H. J. (2008). Cells for bioartificial liver devices: the human hepatoma-derived cell line C3A produces urea but does not detoxify ammonia. *Biotechnol Bioeng*, 99 (3): 644-51.
Miles, L., Heubi, J. E. & Bove, K. E. (2005). Hepatocyte glycogen accumulation in patients undergoing dietary management of urea cycle defects mimics storage disease. *J Pediatr Gastroenterol Nutr*, 40 (4): 471-6.
Misel, M. L., Gish, R. G., Patton, H. & Mendler, M. (2013). Sodium benzoate for treatment of hepatic encephalopathy. *Gastroenterol Hepatol (N Y)*, 9 (4): 219-27.
Mitzner, S. R. (2011). Extracorporeal liver support-albumin dialysis with the Molecular Adsorbent Recirculating System (MARS). *Ann Hepatol*, 10 Suppl 1: 21-8.
Mori, T., Nagai, K., Mori, M., Nagao, M., Imamura, M., Iijima, M. & Kobayashi, K. (2002). Progressive liver fibrosis in late-onset argininosuccinate lyase deficiency. *Pediatr Dev Pathol*, 5 (6): 597-601.
Mosmann, T. (1983). Rapid colorimetric assay for cellular growth and survival: application to proliferation and cytotoxicity assays. *J Immunol Methods*, 65 (1-2): 55-63.
Nagamani, S. C., Erez, A. & Lee, B. (2012). Argininosuccinate lyase deficiency. *Genet Med*, 14 (5): 501-7.
NCBI. (2015a). *AQP8 aquaporin 8*. National Center for Biotechnology Information. Available at: http://www.ncbi.nlm.nih.gov/gene/343 (accessed: 14.05.2015.).
NCBI. (2015b). *SLCO4A1 solute carrier organic anion transporter family, member 4A1*. National Center for Biotechnology Information. Available at: http://www.ncbi.nlm.nih.gov/gene/28231 (accessed: 14.05.2015).

Nissim, I. (1999). Newer aspects of glutamine/glutamate metabolism: the role of acute pH changes. *Am J Physiol*, 277 (4 Pt 2): 493-7.
Ohtsuka, H., Abe, T., Onogawa, T., Kondo, N., Sato, T., Oshio, H., Mizutamari, H., Mikkaichi, T., Oikawa, M., Rikiyama, T., et al. (2006). Farnesoid X receptor, hepatocyte nuclear factors 1alpha and 3beta are essential for transcriptional activation of the liver-specific organic anion transporter-2 gene. *J Gastroenterol*, 41 (4): 369-77.
Olde Damink, S. W., Deutz, N. E., Dejong, C. H., Soeters, P. B. & Jalan, R. (2002). Interorgan ammonia metabolism in liver failure. *Neurochem Int*, 41 (2-3): 177-88.
Olde Damink, S. W., Jalan, R. & Dejong, C. H. (2009). Interorgan ammonia trafficking in liver disease. *Metab Brain Dis*, 24 (1): 169-81.
Phua, J. & Lee, K. H. (2008). Liver support devices. *Curr Opin Crit Care*, 14 (2): 208-15.
Renga, B., Mencarelli, A., Cipriani, S., D'Amore, C., Zampella, A., Monti, M. C., Distrutti, E. & Fiorucci, S. (2011). The nuclear receptor FXR regulates hepatic transport and metabolism of glutamine and glutamate. *Biochim Biophys Acta*, 1812 (11): 1522-31.
Rojek, A., Fuchtbauer, E. M., Fuchtbauer, A., Jelen, S., Malmendal, A., Fenton, R. A. & Nielsen, S. (2013). Liver-specific Aquaporin 11 knockout mice show rapid vacuolization of the rough endoplasmic reticulum in periportal hepatocytes after amino acid feeding. *Am J Physiol Gastrointest Liver Physiol*, 304 (5): 501-15.
Romero-Gomez, M., Ramos-Guerrero, R., Grande, L., de Teran, L. C., Corpas, R., Camacho, I. & Bautista, J. D. (2004). Intestinal glutaminase activity is increased in liver cirrhosis and correlates with minimal hepatic encephalopathy. *J Hepatol*, 41 (1): 49-54.
Roth, M., Obaidat, A. & Hagenbuch, B. (2012). OATPs, OATs and OCTs: the organic anion and cation transporters of the SLCO and SLC22A gene superfamilies. *Br J Pharmacol*, 165 (5): 1260-87.
Rudman, D., DiFulco, T. J., Galambos, J. T., Smith, R. B., 3rd, Salam, A. A. & Warren, W. D. (1973). Maximal rates of excretion and synthesis of urea in normal and cirrhotic subjects. *J Clin Invest*, 52 (9): 2241-9.
Scott, T. R., Kronsten, V. T., Hughes, R. D. & Shawcross, D. L. (2013). Pathophysiology of cerebral oedema in acute liver failure. *World J Gastroenterol*, 19 (48): 9240-55.
Shulman, M. & Nahmias, Y. (2013). Long-term culture and coculture of primary rat and human hepatocytes. *Methods Mol Biol*, 945: 287-302.
Siller, R., Greenhough, S., Naumovska, E. & Sullivan, G. J. (2015). Small-Molecule-Driven Hepatocyte Differentiation of Human Pluripotent Stem Cells. *Stem Cell Reports*.
Soldatow, V. Y., Lecluyse, E. L., Griffith, L. G. & Rusyn, I. (2013). In vitro models for liver toxicity testing. *Toxicol Res (Camb)*, 2 (1): 23-39.
Soria, L. R., Gradilone, S. A., Larocca, M. C. & Marinelli, R. A. (2009). Glucagon induces the gene expression of aquaporin-8 but not that of aquaporin-9 water channels in the rat hepatocyte. *Am J Physiol Regul Integr Comp Physiol*, 296 (4): 1274-81.
Soria, L. R., Marrone, J., Calamita, G. & Marinelli, R. A. (2013). Ammonia detoxification via ureagenesis in rat hepatocytes involves mitochondrial aquaporin-8 channels. *Hepatology*, 57 (5): 2061-71.

Tang, N., Wang, Y., Wang, X., Zhou, L., Zhang, F., Li, X. & Chen, Y. (2012). Stable overexpression of arginase I and ornithine transcarbamylase in HepG2 cells improves its ammonia detoxification. *J Cell Biochem*, 113 (2): 518-27.

Tsiaoussis, J., Newsome, P. N., Nelson, L. J., Hayes, P. C. & Plevris, J. N. (2001). Which hepatocyte will it be? Hepatocyte choice for bioartificial liver support systems. *Liver Transpl*, 7 (1): 2-10.

Tyakht, A. V., Ilina, E. N., Alexeev, D. G., Ischenko, D. S., Gorbachev, A. Y., Semashko, T. A., Larin, A. K., Selezneva, O. V., Kostryukova, E. S., Karalkin, P. A., et al. (2014). RNA-Seq gene expression profiling of HepG2 cells: the influence of experimental factors and comparison with liver tissue. *BMC Genomics*, 15: 1108.

van Erpecum, K. J., Wang, D. Q., Moschetta, A., Ferri, D., Svelto, M., Portincasa, P., Hendrickx, J. J., Schipper, M. & Calamita, G. (2006). Gallbladder histopathology during murine gallstone formation: relation to motility and concentrating function. *J Lipid Res*, 47 (1): 32-41.

Wagner, M., Fickert, P., Zollner, G., Fuchsbichler, A., Silbert, D., Tsybrovskyy, O., Zatloukal, K., Guo, G. L., Schuetz, J. D., Gonzalez, F. J., et al. (2003). Role of farnesoid X receptor in determining hepatic ABC transporter expression and liver injury in bile duct-ligated mice. *Gastroenterology*, 125 (3): 825-38.

Wang, J. Q., Zhang, L., Tao, X. G., Wei, L., Liu, B., Huang, L. L. & Chen, Y. G. (2013). Tetramethylpyrazine upregulates the aquaporin 8 expression of hepatocellular mitochondria in septic rats. *J Surg Res*, 185 (1): 286-93.

Wang, Q., Wang, Y., Yu, Z., Li, D., Jia, B., Li, J., Guan, K., Zhou, Y., Chen, Y. & Kan, Q. (2014). Ammonia-induced energy disorders interfere with bilirubin metabolism in hepatocytes. *Arch Biochem Biophys*, 555-556: 16-22.

Weiner, I. D. & Verlander, J. W. (2010). Molecular physiology of the Rh ammonia transport proteins. *Curr Opin Nephrol Hypertens*, 19 (5): 471-7.

Wright, G., Noiret, L., Olde Damink, S. W. & Jalan, R. (2011). Interorgan ammonia metabolism in liver failure: the basis of current and future therapies. *Liver Int*, 31 (2): 163-75.

Yaplito-Lee, J., Chow, C. W. & Boneh, A. (2013). Histopathological findings in livers of patients with urea cycle disorders. *Mol Genet Metab*, 108 (3): 161-5.

Zimmermann, A., Bachmann, C. & Baumgartner, R. (1986). Severe liver fibrosis in argininosuccinic aciduria. *Arch Pathol Lab Med*, 110 (2): 136-40.

Zollner, G. & Trauner, M. (2009). Nuclear receptors as therapeutic targets in cholestatic liver diseases. *Br J Pharmacol*, 156 (1): 7-27.

Norwegian University
of Life Sciences

Postboks 5003
NO-1432 Ås, Norway
+47 67 23 00 00
www.nmbu.no